Hydrothermal activity lowers trophic diversity in Antarctic hydrothermal sediments

James B. Bell[1,2,3], William D. K. Reid[4], David A. Pearce[5], Adrian G. Glover[2], Christopher J. Sweeting[4], Jason Newton[6], & Clare Woulds[1]*

[1]School of Geography & Water@Leeds, University of Leeds, LS2 9JT, UK.

[2]Life Sciences Dept., Natural History Museum, Cromwell Rd, London SW7 5BD, UK

[3]Centre for Environment, Fisheries and Aquaculture Science, Lowestoft, NR34 0HT, UK

[4]Marine Sciences- School of Natural and Environmental Sciences, Ridley Building, Newcastle University, NE1 7RU, UK

[5]Applied Sciences, Northumbria University, Newcastle, NE1 8ST, UK

[6]NERC Life Sciences Mass Spectrometry Facility, SUERC, East Kilbride G75 0QF, UK

* E-mail: c.woulds@leeds.ac.uk

Keywords: Stable Isotopes; Trophic Niche; Sedimented; Hydrothermal; Southern Ocean; Microbial; 16S; PLFA

Abstract

Hydrothermal sediments are those in which hydrothermal fluid is discharged through sediments and are one of the least studied deep-sea ecosystems. We present a combination of microbial and biochemical data to assess trophodynamics between and within hydrothermal and background areas of the Bransfield Strait (1050 – 1647m depth). Microbial composition, biomass and fatty acid signatures varied widely between and within hydrothermally active and background sites, providing evidence of diverse metabolic activity. Several species had different feeding strategies and trophic positions between hydrothermally active and inactive areas and stable isotope values of consumers were not consistent with feeding morphology. Niche area and the diversity of microbial fatty acids was lowest at the most hydrothermally active site, reflecting trends in species diversity. Faunal uptake of chemosynthetically produced organics was relatively limited but was detected at both hydrothermal and non-hydrothermal sites, potentially suggesting hydrothermal activity can affect trophodynamics over a much wider area than previously thought.

Section 1. Introduction

Hydrothermal sediment (a.k.a. Sediment-hosted/ sedimented hydrothermal vents), the product of subsurface mixing between hydrothermal fluid and ambient seawater within the sediment, are physically more similar to background deep-sea habitats than they are to high temperature, hard substratum vents (Bemis et al. 2012, Bernardino et al. 2012). This means that, whilst they can host chemosynthetic obligate species, they can also be more easily colonised by non-specialist fauna and potentially offer an important metabolic resource in the nutrient-limited deep-sea (Levin et al. 2009, Dowell et al. 2016). Hydrothermal sediments have also been suggested to act as evolutionary bridges between hard substratum vents and methane seeps (Kiel 2016). To utilise in situ production in hydrothermal sediments, fauna must overcome the environmental stress associated with high-temperature, acidic and toxic conditions (Levin et al. 2013, Gollner et al. 2015). The combination of elevated toxicity and in-situ organic matter (OM) production results in a different complement of ecological niches between hydrothermal and background conditions that elicits compositional changes along a productivity-toxicity gradient (Bernardino et al. 2012, Gollner et al. 2015, Bell et al. 2016b). Hydrothermal sediments offer different relative abundances of chemosynthetic and photosynthetic organic matter, depending upon supply of surface-derived primary productivity and levels of hydrothermal activity (Tarasov et al. 2005). In shallow environments (<200 m depth), where production of chemosynthetic and photosynthetic organic matter sources can co-occur, consumption may still favour photosynthetic OM over chemosynthetic OM as this does not require physiological adaptions to environmental toxicity (Kharlamenko et al. 1995, Tarasov et al. 2005, Sellanes et al. 2011). The limited data available concerning trophodynamics at deep-sea hydrothermal sediments, in the Arctic, indicate that diet composition can vary widely between species (Sweetman et al. 2013).

Hydrothermal sediments host diverse microbial communities (Teske et al. 2002, Kallmeyer & Boetius 2004). Microbial communities are a vital intermediate between inorganic substrates and metazoan consumers, and thus their composition and isotopic signatures are of direct relevance to metazoan food webs. The heat flux associated with hydrothermal activity provides both benefits and constraints to microbial communities (Kallmeyer & Boetius 2004, Teske et al. 2014) as well as accelerating the degradation of organic matter, giving rise to a wide variety of compounds including hydrocarbons and organic acids (Martens 1990, Whiticar & Suess 1990, Dowell et al. 2016). Microbial aggregations are commonly visible on the sediment surface in hydrothermal sediments (Levin et al. 2009, Sweetman et al. 2013, Dowell et al. 2016) but microbial activity also occurs throughout the underlying sediment, occupying a wide range of geochemical and thermal niches (reviewed by Teske et al. 2014). Sedimented chemosynthetic ecosystems may present several sources of organic matter to consumers (Bernardino et al. 2012, Sweetman et al. 2013, Yamanaka et al. 2015) and the diverse microbial assemblages can support a variety of reaction pathways, including methane oxidation, sulphide oxidation, sulphate reduction and nitrogen fixation (Teske et al. 2002, Dekas et al. 2009, Jaeschke et al. 2014). Phospholipid fatty acid (PLFA) analysis can be used to describe recent microbial activity and $\delta^{13}C$ signatures (Boschker & Middelburg 2002, Yamanaka & Sakata 2004, Colaço et al. 2007). Although it can be difficult to ascribe a PLFA to a specific microbial group or process, high relative abundances of certain PLFAs can be strongly indicative of chemoautotrophy (Yamanaka & Sakata 2004, Colaço et al. 2007), and can support an understanding of microbial ecosystem function in hydrothermal sediments (e.g. in western pacific vents, see Yamanaka & Sakata 2004).

Macrofaunal assemblages in Bransfield hydrothermal sediments were strongly influenced by hydrothermal activity (Bell et al. 2016b, Bell et al. 2017). Bacterial mats were widespread across

Hook Ridge, where variable levels of hydrothermal activity were detected (Aquilina et al. 2013). Populations of siboglinid polychaetes (*Sclerolinum contortum* and *Siboglinum* sp.) were found at Hook Ridge and non-hydrothermally active sites (Sahling et al. 2005, Georgieva et al. 2015, Bell et al. 2016b) and can harbour chemoautotrophic endosymbionts (Schmaljohann et al. 1990, Eichinger et al. 2013, Rodrigues et al. 2013).

Stable isotope analysis (SIA) is a powerful tool to assess spatial and temporal patterns in faunal feeding behaviour and has been used to study trophodynamics and resource partitioning in other hydrothermal sediments, predominately in the Pacific (Fry et al. 1991, Levin et al. 2009, Portail et al. 2016). Stable isotopic analyses provide inferential measures of different synthesis pathways and can elucidate a wide range of autotrophic or feeding behaviours. Carbon and sulphur isotopes are used to delineate food sources and nitrogen to estimate trophic position. The signature of source isotope ratios ($\delta^{13}C$ & $\delta^{34}S$) is influenced by the isotopic ratio of the chemical substrate, and the fractionation associated with the metabolic process involved and thus, different fixation pathways can elicit different isotopic signatures, even when derived from a single source (e.g. DIC) (Fry et al. 1991). Possible $\delta^{13}C$ isotopic values of sources in the Bransfield Strait include: ~-40 ‰ for thermogenic methane; ~-27 ‰ for suspended particulate matter or ~-15 ‰ for ice algae (Whiticar & Suess 1990, Mincks et al. 2008, Henley et al. 2012, Young et al. 2013). As an example, *Siboglinum* spp. can use a range of resources, including methane or dissolved organic matter (Southward et al. 1979, Schmaljohann et al. 1990, Thornhill et al. 2008, Rodrigues et al. 2013), making SIA an ideal way in which to examine resource utilisation in these settings (Levin et al. 2009, Soto 2009). We also apply the concept of an isotopic niche (Layman et al. 2007) whereby species or community trophic activity is inferred from the distribution of stable isotopic data in two or three dimensional isotope space.

Hypotheses

We used a combination of microbial diversity data based sequencing and compound specific isotopic analyses and bulk isotopic data from sediment, microbial, macro- and megafaunal samples to investigate resource utilisation, niche partitioning and trophic structure at hydrothermal and background sites in the Bransfield Strait to test the following hypotheses: 1) Chemosynthetic organic matter will be an important food source in hydrothermal sediments; 2) Siboglinid species subsist upon chemosynthetically-derived OM 3) Stable isotope signatures will reflect a-priori functional designations defined by faunal morphology and 4) Fauna will have distinct niches between hydrothermal sites and background areas.

Section 2. Materials and Methods

2.1. Sites and Sampling

Samples were collected; during RRS *James Cook* cruise JC55 in the austral summer of 2011 (Tyler et al. 2011), from three raised edifices along the basin axis (Hook Ridge, the Three Sisters and The Axe) and one off-axis site in the Bransfield Strait (1024 – 1311m depth; Fig. 1; Table 1). We visited two sites of variable hydrothermal activity (Hook Ridge 1 and 2) and three sites where hydrothermal activity was not detected (Three Sisters, the Axe and an Off-Axis site) (Aquilina et al. 2013). Of the two hydrothermal sites, Hook Ridge 2 had higher fluid advection rates and pore fluid temperature but lower concentrations of sulphide and methane (Dählmann et al. 2001, Aquilina et al. 2013, Aquilina et al. 2014).

Samples were collected with a Bowers & Connelly dampened megacorer (1024 – 1311 m depth) and a single Agassiz trawl at Hook Ridge (1647 m depth). With the exception of salps, all microbial and faunal samples presented here were from megacore deployments. For a detailed description of the megacore sampling programme and macrofaunal communities, see Bell et al. (2016b). Sampling consisted of 1 – 6 megacore deployments per site, with 2 – 5 cores pooled per deployment (Bell et al. 2016b). Cores were sliced into 0 – 5 cm and 5 – 10 cm partitions and macrofauna were retained on a 300µm sieve. Residues were preserved in either 80 % ethanol or 10 % buffered formalin initially and then stored in 80% ethanol after sorting (Bell et al. 2016b). Fauna were sorted to species/ morphospecies level (for annelid and bivalve taxa); family level (for peracarids) and higher levels for less abundant phyla (e.g. echiurans). Salps were collected using an Agassiz trawl and samples were immediately picked and frozen at -80 ˚C and subsequently freeze-dried.

144

145 2.2. Microbiology Sequencing

146

147 Samples of surface sediment (0 – 1 cm below seafloor (cmbsf)) were taken from megacores the
148 two Hook Ridge sites and the off-axis site and frozen (-80˚C). DNA was extracted from the
149 sediment by Mr DNA (Shallowater, TX, USA) using an in-house standard 454 pipeline. The
150 resultant sequences were trimmed and sorted using default methods in Geneious (v.9.1.5 with
151 RDP v.2.8 and Krona v.2.0) and analysed in the Geneious '16 Biodiversity Tool'
152 (https://16s.geneious.com/16s/help.html; (Wang et al. 2007, Ondov et al. 2011, Biomatters
153 2014).

154

155 2.3. Phospholipid Fatty Acids

156

157 Samples of 3 – 3.5 g of freeze-dried sediment from Hook Ridge 1 & 2, the off-vent site and the
158 Three Sisters were analysed at the James Hutton Institute (Aberdeen, UK) following the
159 procedure detailed in Main et al. (2015), summarised below. Samples were from the top 1 cm of
160 sediment for all sites except Hook Ridge 2 where sediment was pooled from two core slices (0 –
161 2 cm), due to sample mass limitations. Lipids were extracted following a method adapted from
162 Bligh (1959), using a single phase mixture of chloroform: methanol: citrate buffer (1:2:0.8 v-v:v).
163 Lipids were fractionated using 6 ml ISOLUTE SI SPE columns, preconditioned with 5 ml
164 chloroform. Freeze-dried material was taken up in 400 µL of chloroform; vortex mixed twice and
165 allowed to pass through the column. Columns were washed in chloroform and acetone (eluates
166 discarded) and finally 10 ml of methanol. Eluates were collected, allowed to evaporate under a
167 N_2 atmosphere and frozen (-20 ˚C).

168

169 Fatty acids were derivitised with methanol and KOH to produce fatty acid methyl esters (FAMEs).
170 Samples were taken up in 1 mL of 1:1 (v:v) mixture of methanol and toluene. 1 mL of 0.2 M KOH
171 (in methanol) was added with a known quantity of an internal standard (C19 – nonadecanoic
172 acid), vortex mixed and incubated at 37 ˚C for 15 min. After cooling to room temperature, 2 mL
173 of isohexane:chloroform (4:1 v:v), 0.3 mL of 1 M acetic acid and 2 mL of deionized water was
174 added to each vial. The solution was mixed and centrifuged and the organic phase transferred to
175 a new vial and the remaining aqueous phase was mixed and centrifuged again to further extract
176 the organic phase, which was combined with the previous. The organic phases were evaporated
177 under a N_2 atmosphere and frozen at -20 ˚C.
178
179 Samples were taken up in isohexane to perform gas chromatography-combustion-isotope ratio
180 mass spectrometry (GC-C-IRMS). The quantity and $\delta^{13}C$ values of individual FAMEs were
181 determined using a GC Trace Ultra with combustion column attached via a GC Combustion III to
182 a Delta V Advantage isotope ratio mass spectrometer (Thermo Finnigan, Bremen). The $\delta^{13}C_{VPDB}$
183 values (‰) of each FAME were calculated with respect to a reference gas of CO_2, traceable to
184 IAEA reference material NBS 19 TS-Limestone. Measurement of the Indiana University reference
185 material hexadecanoicacid methyl ester (certified $\delta^{13}C_{VPDB}$ -30.74 ± 0.01‰) gave a value of
186 30.91 ± 0.31‰ (mean ± s. d., n = 51). Combined areas of all mass peaks (m/z 44, 45 and 46),
187 following background correction, were collected for each FAME. These areas, relative to the
188 internal C19:0 standard, were used to quantify the 34 most abundant FAMEs and related to the
189 FAs from which they are derived (Thornton et al. 2011).
190
191 Bacterial biomass was calculated using transfer functions from the total mass of four PLFAs
192 (i14:0, i15:0, a15:0 and i16:0), estimated at 14 % of total bacterial PLFA, which in turn is
193 estimated at 5.6 % of total bacterial biomass (Boschker & Middelburg 2002).

194

195 2.4. Bulk Stable Isotopes

196

197 All bulk isotopic analyses were completed at the East Kilbride Node of the Natural Environment
198 Research Council Life Sciences Mass Spectrometry Facility. Specimens with carbonate structures
199 (e.g. bivalves) were physically decarbonated and all specimens were rinsed in de-ionised water
200 (e.g. to remove soluble precipitates such as sulphates) and cleaned of attached sediment before
201 drying. Specimens dried for at least 24 hours at 50˚C and weighed (mg, correct to 3 d.p.) into tin
202 capsules and stored in a desiccator whilst awaiting SIA. Samples were analysed by continuous
203 flow isotope ratio mass spectrometer using a Vario-Pyro Cube elemental analyser (Elementar),
204 coupled with a Delta Plus XP isotope ratio mass spectrometer (Thermo Electron). Each of the
205 runs of CN and CNS isotope analyses used laboratory standards (Gelatine and two amino acid-
206 gelatine mixtures) as well as the international standard USGS40 (glutamic acid). CNS
207 measurements used the internal standards (MSAG2: (Methanesulfonamide/ Gelatine and M1:
208 Methionine) and the international silver sulphide standards IAEA-S1, S2 and S3. All sample runs
209 included samples of freeze-dried, powdered *Antimora rostrata* (ANR), an external reference
210 material used in other studies of chemosynthetic ecosystems (Reid et al. 2013, Bell et al. 2016a),
211 used to monitor variation between runs and instruments (supplementary file 1). Instrument
212 precision (S.D.) for each isotope measured from ANR was 0.42 ‰, 0.33 ‰ and 0.54 ‰ for
213 carbon, nitrogen and sulphur respectively. The reference samples were generally consistent
214 except in one of the CNS runs, which showed unusual $\delta^{15}N$ measurements (S1), so faunal $\delta^{15}N$
215 measurements from this run were excluded as a precaution. Stable isotope ratios are all reported
216 in delta (δ) per mil (‰) notation, relative to international standards: V-PDB ($\delta^{13}C$); Air ($\delta^{15}N$)
217 and V-CDT ($\delta^{34}S$). Machine error, relative to these standards ranged 0.01 – 0.23 for $\delta^{13}C$, for 0.01
218 – 0.13 $\delta^{15}N$ and 0.13 – 3.04 for $\delta^{34}S$. One of the Sulphur standards (Ag_2S IAEA: S2) had a notable

219 difference from the agreed measurements, suggesting either a compromised standard or poor
220 instrument precision. This error was not observed in other standards, or the reference material
221 used, but given the uncertainty here; only $\delta^{34}S$ differences greater than 3 ‰ are considered as
222 being significant.
223
224 A combination of dual- ($\delta^{13}C$ & $\delta^{15}N$, 319 samples) and tri-isotope ($\delta^{13}C$, $\delta^{15}N$ & $\delta^{34}S$, 83 samples)
225 techniques was used to describe bulk isotopic signatures of 43 species of macrofauna (35 from
226 non-hydrothermal sites, 19 from hydrothermal sites and 11 from both), 3 megafaunal taxa and
227 sources of organic matter. Samples submitted for carbon and nitrogen (CN) analyses were
228 pooled if necessary to achieve an optimal mass of 0.7 mg (± 0.5 mg). Where possible, individual
229 specimens were kept separate in order to preserve variance structure within populations but in
230 some cases, low sample mass meant individuals had to be pooled (from individuals found in
231 replicate deployments). Optimal mass for tri-istope (CNS) measurements was 2.5 mg (± 0.5 mg)
232 and, as with CN analyses, specimens were preferentially submitted as individual samples or
233 pooled if necessary. Samples of freeze-dried sediment from each site were also submitted for
234 CNS analyses (untreated for NS and acidified with 6M HCl for C). Acidification was carried out
235 by repeated washing with acid and de-ionised water.
236
237 Specimens were not acidified. A pilot study, and subsequent results presented here, confirmed
238 that the range in $\delta^{13}C$ measurements between acidified (0.1M and 1.0M HCl) was within the
239 untreated population range, in both polychaetes and peracarids and that acidification did not
240 notably or consistently reduce $\delta^{13}C$ standard deviation (Table 2). In the absence of a large or
241 consistent treatment effect, the low sample mass, (particularly for CNS samples) was dedicated
242 to increasing replication and preserving integrity of $\delta^{15}N$ & $\delta^{34}S$ measurements instead of
243 separating carbon and nitrogen/ sulphur samples (Connolly & Schlacher 2013).

Formalin and ethanol preservation effects can both influence the isotopic signature of a sample (Fanelli et al. 2010, Rennie et al. 2012). Taxa that had several samples of each preservation method from a single site (to minimise intra-specific differences) were examined to determine the extent of isotopic shifts associated with preservation effects. Carbon and nitrogen isotopic differences between ethanol and formalin preserved samples ranged between 0.1 ‰ – 1.4 ‰ and 0.4 ‰ – 2.0 ‰ respectively. Differences across all samples were not significant (Paired t-test, $\delta^{13}C$: $t = 2.10$, $df = 3$, $p = 0.126$ and $\delta^{15}N$: $t=1.14$, $df = 3$, $p = 0.337$). Given the unpredictable response of isotopic signatures to preservation effects (which also cannot be extricated from within-site, intraspecific variation) it was not possible to correct isotopic data (Bell et al. 2016a). This contributed an unavoidable, but generally quite small, source of error in these measurements.

2.5. Statistical Analyses

All analyses were completed in the R statistical environment (R Core Team 2013). CN stable isotopic measurements were divided into those from hydrothermal or non-hydrothermal sites and averaged by taxa and used to construct a Euclidean distance matrix (Valls et al. 2014). A similarity profile routine (SIMPROF, 10 000 permutations, $p = 0.05$, Ward linkage) was applied to the distance matrix in the clustsig package (v1.0) (Clarke et al. 2008, Whitaker & Christmann 2013) to detect significant structure. The resulting cluster assignations were compared to a-priori feeding groups (Bell et al. 2016b) using a Spearman Correlation Test (with 9 999 Monte Carlo resamplings) using the coin package (v1.0-24) (Hothorn et al. 2015). Isotopic signatures of species sampled from both hydrothermal and non-hydrothermal sites were also compared

268 with a one-way ANOVA with Tukey's HSD pairwise comparisons (following a Shapiro-Wilk
269 normality test).
270
271 Mean faunal measurements of $\delta^{13}C$ & $\delta^{15}N$ were used to calculate Layman metrics for each site
272 (Layman et al. 2007), sample-size corrected standard elliptical area (SEAc) and Bayesian
273 posterior draws (SEA.B, mean of 10^5 draws ± 95 % credibility interval) in the SIAR package
274 (v4.2) (Parnell et al. 2010, Jackson et al. 2011). Differences in SEA.B between sites were
275 compared in mixSIAR. The value of p given is the proportion of ellipses from group A that were
276 smaller in area than those from group B (e.g. if p = 0.02, then 2 % of posterior draws from group
277 A were smaller than the group B mean) and is considered to be a semi-quantitative measure of
278 difference in means (Jackson et al. 2011).

279 Section 3. Results

280

281 3.1. Differences in microbial composition along a hydrothermal gradient

282

283 A total of 28,767, 35,490 and 47,870 sequences were obtained from the off-axis site and the
284 hydrothermal sites, Hook Ridge 1 and 2, respectively. Bacteria comprised almost the entirety of
285 each sample, with archaea being detected only in the Hook Ridge 2 sample (< 0.1 % of sequences;
286 Fig. 2). Hook Ridge 1 was qualitatively more similar to the off-axis site than Hook Ridge 2. Both
287 Hook Ridge 1 (hydrothermal) and the off-vent site were dominated by proteobacteria (48 % and
288 61 % of reads respectively; Fig. 2), whereas flavobacteriia dominated Hook Ridge 2 (43 %, 7 –
289 12 % elsewhere) with proteobacteria accounting for a smaller percentage of sequences (36 %;
290 Fig. 2). By sequence abundance, flavobacteriia were the most clearly disparate group between
291 Hook Ridge 2 and the other sites. flavobacteriia were comprised of 73 genera at Hook Ridge 2,
292 60 genera at BOV and 63 genera at HR1, of which 54 genera were shared between all sites. Hook
293 Ridge 2 had 15 unique flavobacteriial genera but these collectively accounted for just 0.9% of
294 reads, indicating that compositional differences were mainly driven by relative abundance,
295 rather than taxonomic richness.

296

297 The most abundant genus from each site was *Arenicella* at BOV and HR1 (7.1 and 5.2 % of reads
298 respectively) and *Aestuariicola* at HR2 (6.9 % of reads) (Table 3). The four most abundant genera
299 at both BOV and HR1 were *Arenicella* (γ-proteobacteria), *Methylohalomonas* (γ-proteobacteria),
300 *Pasteuria* (bacilli) & *Blastopirellula* (planctomycetacia), though not in the same order, and
301 accounted for 17.2% and 16.0 % of reads respectively. The four most abundant genera at HR2,
302 accounting for 20.2 % of reads were *Aestuariicola*, *Lutimonas, Maritimimonas* & *Winogradskyella*

303 (favobacteriia). The genera *Arenicella* and *Pasteuria* were the most relatively abundant across
304 all sites (2.2 % – 7.1 % and 1.7 % – 5.0 % of reads respectively; Table 3).
305
306 3.2. Microbial fatty acids
307
308 A total of 37 sedimentary FAs were identified across all sites, in individual abundances ranging
309 between 0 % – 26.4 % of total FA (Table 4; Supplementary Fig 1). All lipid samples were
310 dominated by saturated and mono-unsaturated fatty acids (SFAs and MUFAs), comprising 91 %
311 – 94 % of FA abundance per site. The most abundant FAs at each site were 16:0 (15.7 % – 26.4 %),
312 16:1ω7c (11.5 % – 20.0 %) and 18:1ω7 (4.8 % – 16.9 %; Table 4). PLFA profiles from each of the
313 non-hydrothermal sites sampled (Off-axis and the Three Sisters, 33 and 34 FAs respectively)
314 were quite similar (Table 4) and shared all but one compound (16:1ω11c, present only at the
315 non-hydrothermal Three Sisters site). Fewer FAs were enumerated from Hook Ridge 1 and 2 (31
316 and 23 respectively), including 3 FAs not observed at the non-hydrothermal sites (br17:0, 10-
317 Me-17:0 & 10-Me-18:0), which accounted for 0.5 % – 1.2 % of the total at these sites. Poly-
318 unsaturated algal biomarkers (20:5ω3 and 22:6 ω3) were only detected at the non-
319 hydrothermal site (0.83 – 1.57 % of total FA abundance). Hook Ridge 2 had the lowest number
320 of FAs and the lowest total FA biomass of any site, though this was due in part to the fact that
321 this sample had to be pooled from the top 2 cm of sediment (top 1cm at other sites). Bacterial
322 biomass was highest at Hook Ridge 1 and ranged 85 mg C m^{-2} – 535 mg C m^{-2} (Table 3).
323
324 PLFA carbon isotopic signatures ranged -56 ‰ to -20 ‰ at non-hydrothermal sites and -42 ‰
325 to -8 ‰ at hydrothermal sites (Table 4). Weighted average $\delta^{13}C$ values were quite similar
326 between the non-hydrothermal sites and Hook Ridge 1 (-30.5 ‰ and -30.1 ‰ respectively), but
327 were heavier at Hook Ridge 2 (-26.9 ‰; Table 4). Several of the FAs identified had a large range

328 in $\delta^{13}C$ between samples (including 16:1ω11t $\delta^{13}C$ range = 17.2 ‰ or 19:1ω8 $\delta^{13}C$ range =
329 19.1 ‰), even between the non-hydrothermal sites (e.g. 18:2ω6, 9, $\Delta\delta^{13}C$ = 24.4; Table 4). Of
330 the 37 FAs, 7 had a $\delta^{13}C$ range of > 10 ‰ but these were comparatively minor and individually
331 accounted for 0 % – 4.9 % of total abundance. Average $\delta^{13}C$ range was 6.3 ‰ and a further 11
332 FAs had a $\delta^{13}C$ range of > 5 ‰, including some of the more abundant FAs, accounting for 36.8 ‰
333 – 46.6 % at each site. FAs with small $\delta^{13}C$ ranges (< 5 ‰) accounted for 44.6 % – 54.4 % of total
334 abundance at each site.
335
336 3.3. Description of bulk isotopic signatures
337
338 Most faunal isotopic signatures were within a comparatively narrow range ($\delta^{13}C$: -30 ‰ to -
339 20 ‰, $\delta^{15}N$: 5 ‰ to 15 ‰ and $\delta^{34}S$: 10 ‰ to 20 ‰) and more depleted isotopic signatures
340 were usually attributable to siboglinid species (Fig. 3). *Siboglinum* sp. (found at all non-
341 hydrothermal sites) had mean $\delta^{13}C$ and $\delta^{15}N$ values of -41.4 ‰ and -8.9 ‰ respectively and
342 *Sclerolinum contortum* (predominately from Hook Ridge 1 but found at both hydrothermal sites)
343 had values of -20.5 ‰ and -5.3‰ respectively. Some non-endosymbiont bearing taxa (e.g.
344 macrofaunal neotanaids from the off-axis site and megafaunal ophiuroids at Hook Ridge 2) also
345 had notably depleted $\delta^{15}N$ signatures (means -3.6‰ to 2.6 ‰ respectively; Fig. 3).
346
347 Isotopic signatures of sediment organic matter were similar between hydrothermal and non-
348 hydrothermal sites for $\delta^{13}C$ and $\delta^{15}N$ but $\delta^{34}S$ was significantly greater at non-hydrothermal
349 sites ($p < 0.05$, Table 5; Fig. 4). Variability was higher in hydrothermal sediments for all isotopic
350 signatures. Faunal isotopic signatures for $\delta^{13}C$ and $\delta^{34}S$ ranged much more widely than sediment
351 signatures and indicate that sediment organics were a mixture of two or more sources of organic
352 matter. A few macrofaunal species had relatively heavy $\delta^{13}C$ signatures that exceeded -20 ‰

353 that suggested either a heavy source of carbon or marine carbonate in residual exoskeletal tissue,
354 particularly for peracarids (~0 ‰). Samples of pelagic salps from Hook Ridge had mean values
355 for $\delta^{13}C$ of -27.4 ‰ (± 0.9) and $\delta^{34}S$ of 21.5 ‰ (± 0.8).
356
357 3.4. Comparing macrofaunal morphology and stable isotopic signatures
358
359 Isotopic data (mean of each species for each of $\delta^{13}C$, $\delta^{15}N$ and $\delta^{34}S$) were used to construct a
360 Euclidean distance matrix and the resultant hierarchy was compared to classifications based
361 upon morphology. Species were assigned to one of four clusters (SIMPROF, p = 0.05;
362 Supplementary Figure 3). No significant correlation between a-priori (based on morphology)
363 and a-posteriori cluster assignations (based on isotopic data) was detected (Spearman
364 Correlation Test: Z = -1.34; N = 43; p = 0.18). Clusters were mainly discriminated based on $\delta^{15}N$
365 values and peracarids were the only taxa to be represented in all of the clusters, indicating
366 relatively high trophic diversity.
367
368 Several taxa found at both hydrothermal and non-hydrothermal sites were assigned to different
369 clusters between sites. A total of eleven taxa were sampled from both hydrothermal and non-
370 hydrothermal regions, of which four were assigned to different clusters at hydrothermal and
371 non-hydrothermal sites. Neotanaids (Peracarida: Tanaidacea) had the greatest Euclidean
372 distance between hydrothermal/ non-hydrothermal samples (11.36), demonstrating clear
373 differences in dietary composition (Fig. 5). All other species were separated by much smaller
374 distances between regions (range: 0.24 to 2.69). Raw $\delta^{13}C$ and $\delta^{15}N$ values were also compared
375 between hydrothermal and non-hydrothermal samples for each species (one-way ANOVA with
376 Tukey HSD pairwise comparisons). Analysis of the raw data indicated that $\delta^{13}C$ signatures were

377 different for neotanaids only and $\delta^{15}N$ were different for neotanaids and an oligochaete species
378 (*Limnodriloides* sp.) (ANOVA, $p < 0.01$, Fig. 5).
379
380 3.5.Community-level trophic metrics
381
382 All site niches overlapped (mean = 50 %, range = 30 – 82 %) and the positions of ellipse centroids
383 were broadly similar for all sites (Table 6; Fig 6). Hydrothermal site ellipse areas were similar
384 but significantly smaller than non-hydrothermal ellipses (SEA.B, $n = 10^5$, $p = < 0.05$). There were
385 no significant differences in ellipse area between any of the non-hydrothermal sites. Ranges in
386 carbon sources (dCr) were higher for non-hydrothermal sites (Table 6) indicating a greater
387 trophic diversity in background conditions. Nitrogen range (dNr, Table 6) was similar between
388 hydrothermal and non-hydrothermal sites suggesting a similar number of trophic levels within
389 each assemblage. All site ellipses had broadly similar eccentricity (degree of extension along long
390 axis), ranging 0.85 – 0.97 (Table 6), however theta (angle of long axis) differed between
391 hydrothermal and non-hydrothermal sites (-1.43 to 1.55 at Hook Ridge, 0.67 to 0.86 at non-
392 hydrothermal sites). Range in nitrogen sources was more influential at hydrothermal sites as
393 *Sclerolinum contortum*, which had very low $\delta^{15}N$ signatures but similar $\delta^{13}C$ values, when
394 compared with non-endosymbiont bearing taxa from the same sites. The strongly depleted $\delta^{13}C$
395 measurements of *Siboglinum* sp. meant that ellipse theta was skewed more towards horizontal
396 (closer to zero) for non-hydrothermal sites.
397

398 Section 4. Discussion

399

400 4.1. Microbial signatures of hydrothermal activity

401

402 Fatty acid profiles at the non-hydrothermal off-axis and three sisters sites indicated similar
403 bacterial biomass. Bacterial biomass varied much more widely at Hook Ridge (Table 4). The
404 Hook Ridge 2 sample is not directly comparable since it was sampled from sediment 0 – 2 cmbsf
405 (rather than 0 – 1 cmbsf, owing to sample mass availability). Organic carbon content, hydrogen
406 sulphide flux and taxonomic diversity were all lower at this site and may support suggestion of
407 a lower overall bacterial biomass (Aquilina et al. 2013, Bell et al. 2016b). The very high bacterial
408 biomass at Hook Ridge 1 suggests a potentially very active bacterial community, comparable to
409 other hydrothermal sediments (Yamanaka & Sakata 2004) but $\delta^{13}C_{org}$ was qualitatively similar
410 to non-hydrothermal sites, implying that chemosynthetic activity was not the dominant source
411 of organic carbon, or that the isotopic signatures of the basal carbon source (e.g. DIC) and the
412 fractionation associated with FA synthesis resulted in similar $\delta^{13}C$ signatures.

413

414 A small number of the more abundant fatty acids had notable differences in relative abundance
415 between hydrothermal and background sites (Table 4). For example, 16:1ω7, which has been
416 linked to sulphur cycling pathways (Colaço et al. 2007) comprised 14.0 % – 15.2 % of abundance
417 at non-hydrothermal sites and 20.0 % – 23.5 % at hydrothermal sites. However, 18:1ω7, also a
418 suggested PLFA linked to thio-oxidation (McCaffrey et al. 1989, Colaço et al. 2007) occurred in
419 lower abundance at hydrothermal sites (4.8 % – 11.1 %) than non-hydrothermal sites (15.9 %
420 – 16.9 %), and was also abundant in deeper areas of the Antarctic shelf (Würzberg et al. 2011).
421 Heavier carbon isotopic signatures (> -15 ‰) are generally associated with rTCA cycle carbon
422 fixation (Hayes 2001, Hugler & Sievert 2011, Reid et al. 2013), suggesting that this pathway may

423 have been active at the hydrothermal sites, albeit at probably quite low rates. Conversely, many
424 of the lightest $\delta^{13}C$ signatures (e.g. 19:1ω8, -56.6 ‰, off-axis site) were associated with the non-
425 hydrothermal sites, although it should be noted that 19:1ω8 has not been definitively linked to
426 a particular bacterial process (Koranda et al. 2013, Dong et al. 2015). Lower FA carbon isotope
427 signatures with small ranges (e.g. -60 ‰ to -50 ‰) could also be indicative of methane cycling,
428 but most FAs at all sites had $\delta^{13}C$ of > -40 ‰. These results further suggest that chemosynthetic
429 activity was relatively limited and support a rejection of hypothesis one, since, although there
430 were differences between sites in PLFAs that are potentially indicative of chemosynthetic
431 activity, these were not necessarily consistent between different PLFAs. The metabolic
432 provenance of several of the more abundant PLFAs is also still uncertain. A number of fatty acids
433 have been linked, though not exclusively, to chemoautotrophy, such as 10-Me-16:0
434 (*Desulfobacter* or *Desulfocurvus,* sulphate reducers) and 18:1ω7 (Yamanaka & Sakata 2004,
435 Colaço et al. 2007, Klouche et al. 2009, Boschker et al. 2014) and their presence may be
436 consistent with the hydrothermal signature of the sediment microbial community. There were
437 notable proportions of compounds normally associated with sulphate-reducing bacteria
438 (Kohring et al. 1994, Boschker et al. 2014). These included iC15:0, aiC15:0, 1C17:0 and aiC17:0,
439 which together constituted ~8-12 % of the FA suite. In addition, C16:1ω5c was relatively
440 abundant (Supplementary figure 1), and minor amounts of 10MeC16:0, C17:1ω8c, and
441 cycloC17:0 were present. These have also been used as indicators of sulphate-reducing bacteria,
442 and sometimes of particular groups (e.g. Guezennec & Fiala-Medioni 1996, Boschker et al. 2014).
443 These compounds indicate the presence of sulphate-reducing bacteria, although perhaps not as
444 the dominant group. Although the FA suite was indicative of active sulphur cycling activity, it
445 remains difficult to be conclusive about the origin of most FAs even those which have been
446 regularly observed in chemosynthetic contexts (e.g. 18:1ω7) may still be abundant elsewhere
447 (Würzberg et al. 2011).

448

449 Together C16:1ω7c and C18:1ω7 accounted for ~25-35% of the total FA suite and, although they
450 can be more generally associated with gram-negative eubacteria, have frequently been linked to
451 sulphur oxidising bacteria in sediment samples (Pond et al. 1998, Yamanaka & Sakata 2004,
452 Boschker et al. 2014). Their dominance of the suite in the Bransfield Strait is similar to sediments
453 from a vent in the Barbados Trench, where together C16:1ω7 and C18:1ω7 contributed up to
454 50% of FAs (Guezennec & Fiala-Medioni 1996).

455

456 Long chain fatty acids (>C22) indicative of land plants (e.g. Yamanaka & Sakata 2004) and typical
457 indicators of marine phytoplankton production (e.g. C20:3ω5 and C22:6ω3) were very minor
458 constituents, never accounting for more than 3% of total PLFA mass and only detected at the
459 non-hydrothermal sites; Off-Vent and Middle Sister. While their low abundance is at least
460 partially accounted for by rapid degradation during sinking through the water column (Veuger
461 et al. 2012), it also suggests that sedimentary FAs were predominantly of bacterial origin,
462 whether that be due to bacterial reworking of photosynthetic organic matter, or in situ
463 production.

464

465 Chemotrophic bacterial sequences, such as *Blastopirellula* (Schlesner 2015) or *Rhodopirellula*
466 (Bondoso et al. 2014) were found at all sites in relatively high abundance, suggesting widespread
467 and active chemosynthesis, though the lack of a particularly dominant bacterial group associated
468 with chemosynthetic activity suggested that the supply of chemosynthetic OM was likely
469 relatively limited. It remains difficult however to determine which FAs these bacterial lineages
470 may be have been synthesising.

471

Some FAs also had marked differences in $\delta^{13}C$ signatures, even where there was strong compositional similarity between sites (i.e. the non-hydrothermal sites). This suggested that either there were differences in the isotopic values of inorganic or organic matter sources or different bacterial metabolic pathways were active. Between the non-hydrothermal sites, these included PUFAs and MUFAs (poly- and mono-unsaturated fatty acids) such as 18:2ω6, 9 ($\Delta\delta^{13}C$ 24.4 ‰) and 19:1ω8 ($\Delta\delta^{13}C$ 19.1 ‰). Differences in PLFA $\delta^{13}C$ between the hydrothermal sites also ranged widely, with the largest differences being associated with PLFAs such as 16:1ω11t ($\Delta\delta^{13}C$ 17.2 ‰) and 10-Me-16:0 ($\Delta\delta^{13}C$ 11.0 ‰). However, it should be stressed that all PLFAs with larger $\delta^{13}C$ differences between sites were comparatively rare and never individually exceeded 5% of total abundance. Microbial signatures, whilst supporting the suggestion of chemosynthetic activity, are not indicative of chemosynthetic OM being the dominant source of organic matter to food webs at any site (hypothesis one). It is not possible to assess from PLFA data the relative importance of chemoautotrophic and photosynthetic OM sources, since PLFAs degrade quickly and therefore surface FA abundances are inevitably underestimated in deep water samples.

4.2. Siboglinids

Both species of infaunal siboglinid (*Sclerolinum contortum* from Hook Ridge and *Siboglinum* sp. from the non-hydrothermal sites) appeared to subsist upon chemosynthetically derived organic matter, as evidenced by their morphology, and also by their strongly ^{15}N-depleted isotopic signatures (see values with $\delta^{15}N$ of < -2 ‰ in Fig. 3). Low $\delta^{15}N$ signatures have also been observed in other siboglinids in a range of hydrothermal settings, such as *Riftia pachyptila* at the East Pacific Rise hard substratum vents (Rau 1981). Diazotrophy has been detected previously in hydrothermal vents and cold seeps, typified by low $\delta^{15}N$ values (e.g. Rau, 1981; Desai et al.,

2013; Wu et al., 2014; (Yamanaka et al. 2015). Diazotrophy in various reducing settings has been found associated with anaerobic oxidation of methane (Dekas et al., 2009), methanotrophy (Mehta & Baross 2006) and (in a non-marine cave) sulphate reduction (Desai et al. 2013). The latter is also consistent with the low $\delta^{34}S$ signatures of both siboglinid species (Fig. 4), but gene expression analysis and/or isotopic tracing would be required to confirm this suggestion. Alternately, low $\delta^{15}N$ signatures may be explained by uptake of ammonium produced through dissimilatory nitrate reduction (Naraoka et al. 2008, Liao et al. 2014, Bennett et al. 2015), or strong isotopic fractionation during utilization of ammonia (Naraoka et al. 2008, Liao et al. 2014, Bennett et al. 2015). Bulk faunal isotopic signatures are inadequate to determine which of these chemosynthesis-related mechanisms is responsible for *Siboglinum* $\delta^{15}N$ values, which would require analysis of the functional genes in the *Siboglinum* endosymbionts.

$\delta^{15}N$ values for both siboglinids ($\delta^{15}N$ *Sclerolinum* = -5.3 ‰ ± 1.0, *Siboglinum* = -8.9 ‰ ± 0.8) indicated reliance upon locally fixed N_2 (Rau 1981, Dekas et al. 2009, Dekas et al. 2014, Wu et al. 2014, Yamanaka et al. 2015), rather than utilisation of sediment organic nitrogen ($\delta^{15}N$ = 5.7 ‰ ± 0.7). These values were also in contrast to the rest of the non-chemosynthetic obligate species, which generally had much heavier $\delta^{15}N$ values. This supports hypothesis two, that the siboglinid species were subsisting upon chemosynthetic OM, most likely supplied by their endosymbionts.

Carbon isotopic signatures in chemosynthetic primary production depend upon the mode of fixation and the initial ^{13}C of the inorganic substrate. *Sclerolinum contortum* $\delta^{13}C$ (-20.5 ‰ ± 1.0 ‰) was depleted in $\delta^{13}C$ relative to Southern Ocean DIC by around 10 ‰ (Henley et al. 2012, Young et al. 2013), giving it a signal within the fractionation range of the reverse tricarboxylic acid cycle (Yorisue et al. 2012) but the concentration and isotopic composition of DIC can undergo considerable alteration in hydrothermal sediments (Walker et al. 2008). Therefore,

without measurements of $\delta^{13}C$ in pore fluid DIC, it was not possible to determine which fixation pathway(s) were being used by *S. contortum* endosymbionts.

Sulphur isotopic signatures in *S. contortum* were very low, and quite variable (-26.7 ‰ ± 3.5 ‰). *Sclerolinum* endosymbionts may have been utilising sulphide either from hydrothermal fluid, microbial sulphate reduction or re-dissolved from hydrothermal precipitates. Mineral sulphide was present at Hook Ridge that ranged between -28.1 ‰ to +5.1 ‰ (Petersen et al. 2004), consistent with the relatively high $\delta^{34}S$ variability in *S. contortum.* Alternatively, sulphide supplied as a result of microbial sulphate reduction (Canfield 2001) may have been the primary source of organic sulphur, similar to that of solemyid bivalves in reducing sediments (mean $\delta^{34}S$ of -30 ‰ to -20 ‰; Vetter and Fry (1998) and in cold seep settings (Yamanaka et al. 2015). Sulphate reduction can also be associated with anaerobic oxidation of methane (Whiticar & Suess 1990, Canfield 2001, Dowell et al. 2016), suggesting that methanotrophic pathways could also have been important at Hook Ridge. (e.g. abundance of *Methylohalomonas*, 2.1 % – 4.3 % of sequences at all sites; Table 3). Although endosymbiont composition data were not available for the Southern Ocean population, *Sclerolinum contortum* is also known from hydrocarbon seeps in the Gulf of Mexico (Eichinger et al. 2013, Eichinger et al. 2014, Georgieva et al. 2015) and the Håkon Mosby mud volcano in the Arctic ocean, where *S. contortum* $\delta^{13}C$ ranged between -48.3 ‰ to -34.9 ‰ (Gebruk et al. 2003) demonstrating that this species can occupy several reducing environments and use a range of chemosynthetic fixation pathways, including sulphide oxidation and methanotrophy (Eichinger et al. 2014, Georgieva et al. 2015).

Siboglinum sp. $\delta^{13}C$ values (mean -41.4 ‰, range -45.7 ‰ to -38.1 ‰, n = 8) corresponded very closely to published values of thermogenic methane (-43 ‰ to -38 ‰) from the Bransfield Strait (Whiticar & Suess 1990), strongly suggesting that methanotrophy was the dominant carbon

547 source for this species. Biogenic methane, although present in the Bransfield Strait, typically has
548 much lower $\delta^{13}C$ values (Whiticar 1999, Yamanaka et al. 2015), indicating a hydrothermal/
549 thermogenic source of methane in the Bransfield Strait (Whiticar & Suess 1990). Sulphur
550 isotopic signatures were also very low in *Siboglinum* sp. ($\delta^{34}S$ -22.9 ‰, one sample from 15
551 pooled individuals from the off-axis site), the lowest measurement of $\delta^{34}S$ reported for this genus
552 (Schmaljohann & Flügel 1987, Rodrigues et al. 2013). Methanotrophy in *Siboglinum* spp. has
553 been previously documented at seeps in the NE Pacific (Bernardino & Smith 2010) and
554 Norwegian margin ($\delta^{13}C$ = -78.3 ‰ to -62.2 ‰) (Schmaljohann et al. 1990) and in Atlantic mud
555 volcanoes ($\delta^{13}C$ range -49.8 ‰ to -33.0 ‰) (Rodrigues et al. 2013). Rodrigues et al. (2013) also
556 reported a greater range in $\delta^{15}N$ than observed in the Bransfield siboglinids ($\delta^{15}N$ -1.3 ‰ to
557 12.2 ‰ and -10.2 ‰ to -7.6 ‰ respectively). This suggests that, in comparison to *Siboglinum*
558 spp. in Atlantic Mud volcanoes, which seemed to be using a mixture of organic matter sources
559 (Rodrigues et al. 2013), the Bransfield specimens relied much more heavily upon a single OM
560 source, suggesting considerable trophic plasticity in this genus worldwide.
561
562 Off-vent methanotrophy, using thermogenic methane, potentially illustrates an indirect
563 dependence upon hydrothermalism (Whiticar & Suess 1990). Sediment methane production is
564 thought to be accelerated by the heat flux associated with mixing of hydrothermal fluid in
565 sediment (Whiticar & Suess 1990) and sediment and *Siboglinum* isotopic data suggest that the
566 footprint of hydrothermal influence may be much larger than previously recognised, giving rise
567 to transitional environments (Bell et al. 2016a, Levin et al. 2016). Clear contribution of methane-
568 derived carbon to consumer diets was limited predominately to neotanaids, consistent with the
569 relatively small population sizes (64 ind. m^2– 159 ind. m^2) of *Siboglinum* sp. observed in the
570 Bransfield Strait (Bell et al. 2016b).
571

572 4.3. Organic Matter Sources

573

574 Pelagic salps, collected from an Agassiz trawl at Hook Ridge (1647m), were presumed to most
575 closely represent a diet of entirely surface-derived material and were more depleted in ^{13}C and
576 more enriched in ^{34}S than were sediments (Salp $\delta^{13}C$ = -27.4 ‰ & $\delta^{34}S$ = 20.1; Hook Ridge
577 sediment $\delta^{13}C$ = -26.2 ‰ & $\delta^{34}S$ = 14.3) Salp carbon isotopic signatures were also lighter than
578 the majority of macrofauna or sedimentary organic carbon, both at Hook Ridge and the non-
579 hydrothermal sites (Fig. 3) and similar to other suspension feeding fauna in the Bransfield Strait
580 (Elias-Piera et al. 2013).

581

582 Fauna with more depleted $\delta^{34}S$/ more enriched $\delta^{13}C$ values were likely to have derived at least
583 a small amount of their diet from chemosynthetic sources (potentially indirectly through non-
584 selective consumption of detrital OM), both at hydrothermal and background regions (Bell et al.
585 2017). Carbon and sulphur isotopic measurements indicated mixed sources for most consumers
586 between chemosynthetic OM and surface-derived photosynthetic OM. The low content of algal
587 biomarkers (particularly at the hydrothermal sites) suggests that phytodetritus was probably
588 quite degraded and thus challenging to detect using short-lived fatty acids. However, the
589 Bransfield Strait can be subject to substantial export production and it is probable that surface
590 production contributes much more to seafloor OM than is evident from the fatty acid
591 composition. Non-hydrothermal sediments were more enriched in ^{34}S than hydrothermal
592 sediments, an offset that probably resulted from greater availability of lighter sulphur sources
593 such as sulphide oxidation at Hook Ridge, even if surface-derived OM remained the dominant
594 source of organic matter at the hydrothermal sites (Bell et al. 2017).

595

596 Samples of bacterial mat could not be collected during JC55 (Tyler et al. 2011) and without these
597 endmember measurements, it was not possible to quantitatively model resource partitioning in
598 the Bransfield Strait using isotope mixing models (Phillips et al. 2014). Bacterial mats from high-
599 temperature vents in the Southern Ocean had $\delta^{34}S$ values of 0.8 ‰ (Reid et al. 2013) and at
600 sedimented areas of the Loki's Castle hydrothermal vents in the Arctic Ocean has $\delta^{34}S$ values of
601 -4.9 ‰ (Bulk sediment; Jaeschke et al. 2014). Therefore it is probable that low faunal $\delta^{34}S$ values
602 represent a contribution of chemosynthetic OM (from either siboglinid tissue or free-living
603 bacteria). Inorganic sulphur can also be a source to consumers when sulphide is utilised by free
604 living bacteria ($\delta^{34}S$ ranged -7.3 ‰ to 5.4 ‰; Erickson et al. (2009)) and, although we could not
605 analyse the $\delta^{34}S$ of fluid sulphide, sulphide crusts have been found at Hook Ridge and may
606 provide a proxy for typical isotopic composition ($\delta^{34}S$ -28.1 ‰ to 5.1 ‰; Petersen et al. (2004)).
607 There were several species (e.g. Tubificid oligochaetes) that had moderately depleted $\delta^{34}S$
608 signatures, such as *Limnodriloides* sp. ($\delta^{34}S$ 7.6 ‰ at hydrothermal sites, -1.2 ‰ at non-
609 hydrothermal sites, Fig. 4) further supporting the hypothesis of different trophic positions
610 between hydrothermal/ non-hydrothermal regions (hypothesis two). This provides evidence of
611 coupled anaerobic oxidation of methane/ sulphate reduction but overall, the contribution of
612 $\delta^{34}S$-depleted bacterial production did not seem widespread (further rejecting hypothesis four).
613
614 Without samples of all OM sources we cannot quantitatively assert that faunal utilisation of
615 chemosynthetic OM was low in the Bransfield Strait. Although isotopic data were consistent with
616 several OM sources, it seemed unlikely that chemosynthetic OM was a dominant source of OM
617 to the vast majority of taxa. The apparently limited consumption of chemosynthetic OM
618 suggested that either it was not widely available (e.g. patchy or low density of endosymbiont-
619 bearing fauna (Bell et al. 2016b)), or that the ecological stress associated with feeding in areas

620 of in situ production was a significant deterrent to many species (Bernardino et al. 2012, Levin
621 et al. 2013).
622
623 4.4. A-priori vs. a-posteriori trophic groups
624
625 Classifications based upon morphology did not prove to be an accurate predictor of isotopic data,
626 suggesting that faunal behaviour is potentially more important in determining dietary
627 composition than morphology (e.g. having/ lacking jaws). Peracarid species that possessed
628 structures adapted to a motile, carnivorous lifestyle were assigned to a carnivore/ scavenger
629 guild (Bell et al. 2016b) and were distributed throughout the food web both at hydrothermal
630 sites and background regions, indicating more diverse feeding strategies than expected. Taxa
631 presumed to be deposit feeders (largely annelids) also had a large range of $\delta^{15}N$ values. This may
632 reflect the consumption of detritus from both 'fresh' and more recycled/ refractory OM sources
633 as observed in other non-hydrothermal sedimented deep-sea habitats (Iken et al. 2001, Reid et
634 al. 2012) or reflect variability in trophic discrimination related to diet quality (Adams & Sterner
635 2000). A range of foraminifera have now been shown to utilise denitrification which results in
636 them having heavier $\delta^{15}N$ values (Pina-Ochoa et al. 2010, Jeffreys et al. 2015). The result is high
637 $\delta^{15}N$ values in taxa without predatory morphology (e.g. oligochaetes). Tubificid oligochaetes had
638 higher $\delta^{15}N$ values at the hydrothermal sites, suggesting that they fed upon more recycled
639 organic matter, possibly owing to greater microbial activity at hydrothermal sites.
640
641 Several taxa (e.g. ophiuroids at Hook Ridge) had low $\delta^{15}N$ values, relative to sediment OM,
642 suggesting preferential consumption of chemosynthetic OM (Rau 1981, Dekas et al. 2014). In
643 these taxa, it is likely that the widespread, but patchy bacterial mats or *Sclerolinum* populations
644 at Hook Ridge (Aquilina et al. 2013) were an important source of organic matter. Fauna from the

non-hydrothermal sites with low $\delta^{15}N$ (e.g. neotanaids) were likely subsisting in part upon siboglinid tissue (*Siboglinum* sp.). There were no video transects over the off-axis site but footage of the Three Sisters, which was similar in macrofaunal composition (Bell et al. 2016b), did not reveal bacterial mats (Aquilina et al. 2013), hence it is unlikely that these were an important resource at non-hydrothermal sites.

It is clear that some fauna can exhibit a degree of trophic plasticity, depending upon habitat (supporting hypothesis four). This is consistent with other hydrothermal sediments where several taxa (e.g. *Prionospio* sp. – Polychaeta: Spionidae) had different isotopic signatures, depending upon their environment (Levin et al. 2009), demonstrating differential patterns in resource utilisation. Alternatively, there could have been different $\delta^{15}N$ baselines between sites, though if these differences were significant, we argue that it likely that more species would have had significant differences in tissue $\delta^{15}N$. Conversely, samples of *Aurospio foodbancsia* at both hydrothermal and non-hydrothermal sites had broadly similar $\delta^{15}N$ values to that of the west Antarctic Peninsula; 8.1 ‰ and 7.9 ‰ respectively, albeit with a higher variability (Mincks et al. 2008). $\delta^{13}C$ values of *Aurospio* were also broadly similar, implying that this species occupied a detritivorous trophic niche, irrespective of environmental conditions.

4.5. Impact of hydrothermal activity on community trophodynamics

Standard ellipse area was lower at Hook Ridge than elsewhere (Table 6), analogous to trends in macrofaunal diversity and abundance in the Bransfield Strait (Bell et al. 2016b) and changes in SEA.B along a gradient of methane flux at vent and seep ecosystems in the Guaymas Basin (Portail et al. 2016). This demonstrates that at community level, ellipse area can be associated with other macrofaunal assemblage characteristics. Concurrent decline in niche area and alpha

diversity is consistent with the concept that species have finely partitioned niches and greater total niche area permits higher biodiversity (McClain & Schlacher 2015). This relationship may also suggest that the influence of disturbance gradients created by hydrothermalism can result in an impoverished community (McClain & Schlacher 2015, Bell et al. 2016b). Productivity-diversity relationships, whereby higher productivity sustains higher diversity, have also been suggested for deep-sea ecosystems (McClain & Schlacher 2015, Woolley et al. 2016) this is not supported by the Bransfield Strait sites (Bell et al. 2017). We suggest that, in the Bransfield Strait, the environmental toxicity in hydrothermal sediments (from differences in temperature and porewater chemistry) causes a concomitant decline in both trophic and species diversity (Bell et al. 2016b), in spite of the potential for increased localised production (Bell et al. 2017). However, we acknowledge that, owing to the high small-scale habitat heterogeneity apparent from video imagery over the hydrothermally influenced area, that it is likely that the contribution of chemosynthetic organic matter varies widely over 10s of metres at Hook Ridge.

Community-based trophic metrics (Layman et al. 2007) indicated that, although measures of dispersion within sites were relatively similar between hydrothermal sites and background areas (Table 6), trophic diversity, particularly in terms of range of carbon sources (dCr) and total hull area (TA) were higher at background sites, owing to the more depleted carbon and nitrogen signatures of *Siboglinum* spp.. It is still unclear whether the assemblage isotopic niche really corresponds to its actualised trophic niche and, although the niche space was smaller at the hydrothermal sites, the potential for different trophic strategies was still potentially greater (Bell et al. 2017).

Section 5. Conclusions

In this study, we demonstrate the influence of sediment-hosted hydrothermal activity upon trophodynamics and microbial populations. Low activity hydrothermal microbiota were more similar to the non-hydrothermal site than to high activity populations, illustrating the effect of ecological gradients upon deep-sea microbial diversity. Despite widespread bacterial mats, and populations of hydrothermal-endemic macrofauna, utilisation of chemosynthetic OM amongst non-specialist macro- and megafauna seemed relatively low, with a concomitant decline in trophic diversity with increasing hydrothermal activity. Morphology was also not indicative of trophic relationships, demonstrating the effects of differential resource availability and behaviour. We suggest that, because these sedimented hydrothermal sites are insufficiently active to host large populations of vent-endemic megafauna, the transfer of chemosynthetic organic matter into the metazoan food web is likely to be more limited than in other similar environments.

6. Acknowledgements

JBB was funded by a NERC PhD Studentship (NE/L501542/1). This work was funded by the NERC ChEsSo consortium (Chemosynthetically-driven Ecosystems South of the Polar Front, NERC Grant NE/DOI249X/I). Elemental analyses were funded by the NERC Life Sciences Mass Spectrometry Facility (Proposal no. EK234-13/14). We thank Barry Thornton and the James Hutton Laboratory, Aberdeen for processing the PLFA samples. We also thank Will Goodall-Copestake for assistance in processing the 16S sequence data. We are grateful to the Master and Crew of RRS *James Cook* cruise 055 for technical support and the Cruise Principal Scientific Officer Professor Paul Tyler.

7. Ethics Statement

In accordance with the Antarctic Act (1994) and the Antarctic Regulations (1995), necessary permits (S5-4/2010) were acquired from the South Georgia and South Sandwich Islands Government.

8. Author contributions

Conceived and designed the sampling programme: WDKR, DAP, AGG, CJS & CW. Sample laboratory preparation and isotopic analyses: JBB, JN & CJS. Microbial sequencing: DAP. Statistical analyses: JBB. Produced figures: JBB. Wrote the paper: JBB, CW & WDKR, with contributions and comments from all other authors.

729 9. References

730

731 Adams TS, Sterner RW (2000) The effect of dietary nitrogen content on trophic level ^{15}N
732 enrichment. Limnology & Oceanography 45:601-607
733 Aquilina A, Connelly DP, Copley JT, Green DR, Hawkes JA, Hepburn L, Huvenne VA, Marsh L, Mills
734 RA, Tyler PA (2013) Geochemical and Visual Indicators of Hydrothermal Fluid Flow
735 through a Sediment-Hosted Volcanic Ridge in the Central Bransfield Basin (Antarctica).
736 Plos One 8:e54686
737 Aquilina A, Homoky WB, Hawkes JA, Lyons TW, Mills RA (2014) Hydrothermal sediments are a
738 source of water column Fe and Mn in the Bransfield Strait, Antarctica. Geochimica et
739 Cosmochimica Acta 137:64-80
740 Bell JB, Aquilina A, Woulds C, Glover AG, Little CTS, Reid WDK, Hepburn LE, Newton J, Mills RA
741 (2016a) Geochemistry, faunal composition and trophic structure at an area of weak
742 methane seepage on the southwest South Georgia margin. Royal Society Open Science 3
743 Bell JB, Woulds C, Brown LE, Little CTS, Sweeting CJ, Reid WDK, Glover AG (2016b) Macrofaunal
744 ecology of sedimented hydrothermal vents in the Bransfield Strait, Antarctica. Frontiers
745 in Marine Science 3:32
746 Bell JB, Woulds C, van Oevelen D (2017) Hydrothermal activity, functional diversity and
747 chemoautotrophy are major drivers of seafloor carbon cycling. Scientific reports 7
748 Bemis K, Lowell R, Farough A (2012) Diffuse Flow On and Around Hydrothermal Vents at Mid-
749 Ocean Ridges. Oceanography 25:182-191
750 Bennett SA, Dover CV, Breier JA, Coleman M (2015) Effect of depth and vent fluid composition
751 on the carbon sources at two neighboring deep-sea hydrothermal vent fields (Mid-
752 Cayman Rise). Deep Sea Research Part I: Oceanographic Research Papers 104:122-133
753 Bernardino AF, Levin LA, Thurber AR, Smith CR (2012) Comparative Composition, Diversity and
754 Trophic Ecology of Sediment Macrofauna at Vents, Seeps and Organic Falls. Plos ONE
755 7:e33515
756 Bernardino AF, Smith CR (2010) Community structure of infaunal macrobenthos around
757 vestimentiferan thickets at the San Clemente cold seep, NE Pacific. Marine Ecology-an
758 Evolutionary Perspective 31:608-621
759 Biomatters (2014) Geneious.
760 Bligh EG (1959) A rapid method of total lipid extration and purification. Canadian Journal of
761 Biochemistry and Phsiology 37:911-917
762 Bondoso J, Albuquerque L, Lobo-da-Cunha A, da Costa MS, Harder J, Lage OM (2014)
763 Rhodopirellula lusitana sp. nov. and Rhodopirellula rubra sp. nov., isolated from the
764 surface of macroalgae. Syst Appl Microbiol 37:157-164
765 Boschker HT, Middelburg JJ (2002) Stable isotopes and biomarkers in microbial ecology. FEMS
766 Microbiology Ecology 40:85-95
767 Boschker HT, Vasquez-Cardenas D, Bolhuis H, Moerdijk-Poortvliet TW, Moodley L (2014)
768 Chemoautotrophic carbon fixation rates and active bacterial communities in intertidal
769 marine sediments. PLoS One 9:e101443
770 Canfield DE (2001) Isotope fractionation by natural populations of sulfate-reducing bacteria.
771 Geochimica Et Cosmochimica Acta 65:1117-1124
772 Clarke KR, Somerfield PJ, Gorley RN (2008) Testing of null hypotheses in exploratory community
773 analyses: similarity profiles and biota-environment linkage. Journal of Experimental
774 Marine Biology and Ecology 366:56-69

775 Colaço A, Desbruyères D, Guezennec J (2007) Polar lipid fatty acids as indicators of trophic
776 associations in a deep-sea vent system community. Marine Ecology 28:15-24
777 Connolly RM, Schlacher TA (2013) Sample acidification significantly alters stable isotope ratios
778 of sulfur in aquatic plants and animals. Marine Ecology Progress Series 493:1-8
779 Dählmann A, Wallman K, Sahling H, Sarthou G, Bohrmann G, Petersen S, Chin CS, Klinkhammer
780 GP (2001) Hot vents in an ice-cold ocean: Indications for phase separation at the
781 southernmost area of hydrothermal activity, Bransfield Strait, Antarctica. Earth and
782 Planetary Science Letters 193:381-394
783 Dekas AE, Chadwick GL, Bowles MW, Joye SB, Orphan VJ (2014) Spatial distribution of nitrogen
784 fixation in methane seep sediment and the role of the ANME archaea. Environ Microbiol
785 16:3012-3029
786 Dekas AE, Poretsky RS, Orphan VJ (2009) Deep-sea archaea fix and share nitrogen in methane-
787 consuming microbial consortia. Science 326:422-426
788 Desai MS, Assig K, Dattagupta S (2013) Nitrogen fixation in distinct microbial niches within a
789 chemoautotrophy-driven cave ecosystem. Isme Journal 7:2411-2423
790 Dong L-J, Sun Z-K, Gao Y, He W-M (2015) Two-year interactions between invasive Solidago
791 canadensis and soil decrease its subsequent growth and competitive ability. Journal of
792 Plant Ecology:rtv003
793 Dowell F, Cardman Z, Dasarathy S, Kellerman M, Lipp JS, Ruff SE, Biddle JF, McKay L, MacGregor
794 BJ, Lloyd KG, Albert DB, Mendlovitz H, Hinrichs KU, Teske A (2016) Microbial
795 communities in methane- and short chain alkane- rich hydrothermal sediments of
796 Guaymas Basin. Frontiers in microbiology
797 Eichinger I, Hourdez S, Bright M (2013) Morphology, microanatomy and sequence data of
798 *Sclerolinum contortum* (Siboglindae, Annelida) of the Gulf of Mexico. Organisms Diversity
799 & Evolution 13:311-329
800 Eichinger I, Schmitz-Esser S, Schmid M, Fisher CR, Bright M (2014) Symbiont-driven sulfur
801 crystal formation in a thiotrophic symbiosis from deep-sea hydrocarbon seeps. Environ
802 Microbiol Rep 6:364-372
803 Elias-Piera F, Rossi S, Gili JM, Orejas C (2013) Trophic ecology of seven Antarctic gorgonian
804 species. Marine Ecology Progress Series 477:93-106
805 Erickson KL, Macko SA, Van Dover CL (2009) Evidence for a chemotrophically based food web
806 at inactive hydrothermal vents (Manus Basin). Deep Sea Research Part II: Topical Studies
807 in Oceanography 56:1577-1585
808 Fanelli E, Cartes JE, Enric J, Papiol V, Rumolo P, Sprovieri M (2010) Effects of preservation on the
809 δ13C and δ15N values of deep sea macrofauna. Journal of Experimental Marine Biology
810 and Ecology 395:93-97
811 Fry B, Jannasch HW, Molyneaux SJ, Wirsen CO, Muramoto JA, King S (1991) Stable Isotope
812 Studies of the Carbon Nitrogen and Sulfur Cycles in the Black Sea and the Cariaco Trench.
813 Deep-Sea Research Part A Oceanographic Research Papers 38:S1003-S1020
814 Gebruk A, Krylova E, Lein A, Vinogradov G, Anderson E, Pimenov N, Cherkashev G, Crane K
815 (2003) Methane seep community of the Håkon Mosby mud volcano (the Norwegian Sea):
816 composition and trophic aspects. Sarsia: North Atlantic Marine Science 88:394-403
817 Georgieva M, Wiklund H, Bell JB, Eilersten MH, Mills RA, Little CTS, Glover AG (2015) A
818 chemosynthetic weed: the tubeworm *Sclerolinum contortum* is a bipolar, cosmopolitan
819 species. BMC Evolutionary Biology 15:280
820 Gollner S, Govenar B, Fisher CR, Bright M (2015) Size matters at deep-sea hydrothermal vents:
821 different diversity and habitat fidelity patterns of meio- and macrofauna. Marine Ecology
822 Progress Series 520:57-66

Guezennec J, Fiala-Medioni A (1996) Bacterial abundance and diversity in the Barbados Trench determined by phospholipid analysis. Microbiology Ecology 19:83-93
Hayes JM (2001) Fractionation of carbon and hydrogen isotopes in biosynthetic processes. Reviews in Mineralogy & Geochemistry 43:225-277
Henley SF, Annett AL, Ganeshram RS, Carson DS, Weston K, Crosta X, Tait A, Dougans J, Fallick AE, Clarke A (2012) Factors influencing the stable carbon isotopic composition of suspended and sinking organic matter in the coastal Antarctic sea ice environment. Biogeosciences 9:1137-1157
Hothorn T, van de Wiel MA, Zeilis A (2015) Package 'Coin': Conditional Inference Procedures in a Permutation Test Framework. cranr-projectorg
Hugler M, Sievert SM (2011) Beyond the Calvin cycle: autotrophic carbon fixation in the ocean. Annual review of marine science 3:261-289
Iken K, Brey T, Wand U, Voight J, Junghans P (2001) Trophic relationships in the benthic community at Porcupine Abyssal Plain (NE Atlantic): a stable isotope analysis. Progress in Oceanography 50:383-405
Jackson AL, Inger R, Parnell AC, Bearhop S (2011) Comparing isotopic niche widths among and within communities: SIBER - Stable Isotope Bayesian Ellipses in R. The Journal of animal ecology 80:595-602
Jaeschke A, Eickmann B, Lang SQ, Bernasconi SM, Strauss H, Fruh-Green GL (2014) Biosignatures in chimney structures and sediment from the Loki's Castle low-temperature hydrothermal vent field at the Arctic Mid-Ocean Ridge. Extremophiles 18:545-560
Jeffreys RM, Fisher EH, Gooday AJ, Larkin KE, Billett DSM, Wolff GA (2015) The trophic and metabolic pathways of foraminifera in the Arabian Sea: evidence from cellular stable isotopes. Biogeosciences 12:1781-1797
Kallmeyer J, Boetius A (2004) Effects of Temperature and Pressure on Sulfate Reduction and Anaerobic Oxidation of Methane in Hydrothermal Sediments of Guaymas Basin. Applied and environmental microbiology 70:1231-1233
Kharlamenko VI, Zhukova NV, Khotimchenko SV, Svetashev VI, Kamenev GM (1995) Fatty-acids as markers of food sources in a shallow-water hydrothermal ecosystem (Kraternaya Bight, Yankich island, Kurile Islands). Marine Ecology Progress Series 120:231-241
Kiel S (2016) A biogeographic network reveals evolutionary links between deep-sea hydrothermal vent and methane seep faunas. Proceedings of the Royal Society B: Biological Sciences 283
Klinkhammer GP, Chin CS, Keller RA, Dahlmann A, Sahling H, Sarthou G, Petersen S, Smith F (2001) Discovery of new hydrothermal vent sites in Bransfield Strait, Antarctica. Earth and Planetary Science Letters 193:395-407
Klouche N, Basso O, Lascourréges J-F, Cavol J-L, Thomas P, Fauque G, Fardeau M-L, Magot M (2009) Desulfocurvus vexinensis gen. nov., sp. nov., a sulfate-reducing bacterium isolated from a deep subsurface aquifer. International Journal of Systematic and Evolutionary Microbiology 30:3100-3104
Kohring L, Ringelberg D, Devereuk R, Stahl DA, Mittelman MW, White DC (1994) Comparison of phylogenetic relationships based on phospholipid fatty acid profiles and ribosomal RNA sequence similarities among dissimiltory sulfate-reducing bacteria. Fems Microbiology Letters 119:303-308
Koranda M, Kaiser C, Fuchslueger L, Kitzler B, Sessitsch A, Zechmeister-Boltenstern S, Rickhter A (2013) Fungal and bacterial utilization of organic substrates depends on substrate complexity and N availability. In: Dieckmann U (ed). International Institute for Applied Systems Analysis, Laxenburg, Austria

871 Layman CA, Arrington DA, Montaña CG, Post DM (2007) Can Stable Isotope Ratios Provide For
872 Community-Wide Measures of Trophic Structure? Ecology 88:42-48
873 Levin LA, Baco AR, Bowden D, Colaço A, Cordes E, Cunha MR, Demopoulos A, Gobin J, Grupe B,
874 Le J, Metaxas A, Netburn A, Rouse GW, Thurber AR, Tunnicliffe V, Van Dover C, Vanreusel
875 A, Watling L (2016) Hydrothermal Vents and Methane Seeps: Rethinking the Sphere of
876 Influence. Frontiers in Marine Science 3:72
877 Levin LA, Mendoza GF, Konotchick T, Lee R (2009) Macrobenthos community structure and
878 trophic relationships within active and inactive Pacific hydrothermal sediments. Deep
879 Sea Research Part II: Topical Studies in Oceanography 56:1632-1648
880 Levin LA, Ziebis W, Mendoza GF, Bertics VJ, Washington T, Gonzalez J, Thurber AR, Ebbed B, Lee
881 RW (2013) Ecological release and niche partitioning under stress: Lessons from
882 dorvilleid polychaetes in sulfidic sediments at methane seeps. Deep-Sea Research Part II-
883 Topical Studies in Oceanography 92:214-233
884 Liao L, Wankel SD, Wu M, Cavanaugh CM, Girguis PR (2014) Characterizing the plasticity of
885 nitrogen metabolism by the host and symbionts of the hydrothermal vent
886 chemoautotrophic symbioses Ridgeia piscesae. Mol Ecol 23:1544-1557
887 Main CE, Ruhl HA, Jones DOB, Yool A, Thornton B, Mayor DJ (2015) Hydrocarbon contamination
888 affects deep-sea benthic oxygen uptake and microbial community composition. Deep Sea
889 Research Part I: Oceanographic Research Papers 100:79-87
890 Martens CS (1990) Generation of short chain organic acid anions in hydrothermally altered
891 sediments of the Guaymas Basin, Gulf of California. Applied Geochemistry 5:71-76
892 McCaffrey MA, Farrington JW, Repeta DJ (1989) Geo-chemical implications of the lipid
893 composition of *Thioploca* spp. from the Peru upwelling region - 15°S. Organic
894 Geochemistry 14
895 McClain CR, Schlacher TA (2015) On some hypotheses of diversity of animal life at great depths
896 on the sea floor. Marine Ecology:12288
897 Mehta MP, Baross JA (2006) Nitrogen Fixation at 92°C by a Hydrothermal Vent Archaeon. Science
898 314:1783-1786
899 Mincks SL, Smith CR, Jeffreys RM, Sumida PYG (2008) Trophic structure on the West Antarctic
900 Peninsula shelf: Detritivory and benthic inertia revealed by δ13C and δ15N analysis. Deep
901 Sea Research Part II: Topical Studies in Oceanography 55:2502-2514
902 Naraoka H, Naito T, Yamanaka T, Tsunogai U, Fujikura K (2008) A multi-isotope study of deep-
903 sea mussels at three different hydrothermal vent sites in the northwestern Pacific.
904 Chemical Geology 255:25-32
905 Ondov BD, Bergman NH, Phillippy AM (2011) Interactive metagenomic visualization in a Web
906 browser. BMC Bioinformatics 30:385
907 Parnell AC, Inger R, Bearhop S, Jackson AL (2010) Source partitioning using stable isotopes:
908 coping with too much variation. PLoS One 5:e9672
909 Petersen S, Herzig PM, Schwarz-Schampera U, Hannington MD, Jonasson IR (2004)
910 Hydrothermal precipitates associated with bimodal volcanism in the Central Bransfield
911 Strait, Antarctica. Mineralium Deposita 39:358-379
912 Phillips DL, Inger R, Bearhop S, Jackson AL, Moore JW, Parnell AC, Semmens BX, Ward EJ (2014)
913 Best practices for use of stable isotope mixing models in food-web studies. Canadian
914 Journal of Zoology 92:823-835
915 Pina-Ochoa E, Koho KA, Geslin E, Risgaard-Petersen N (2010) Survival and life strategy of the
916 foraminiferan *Globobulimina turgida* though nitrate storage and denitrification. Marine
917 Ecology Progress Series 417:39-49
918 Pond DW, Bell MV, Dixon DR, Fallick AE, Segonzac M, Sargent JR (1998) Stable-Carbon-Isotope
919 Composition of Fatty Acids in Hydrothermal Vent Mussels Containing Methanotrophic

and Thiotrophic Bacterial Endosymbionts. Applied and environmental microbiology 64:370-375
Portail M, Olu K, Dubois SF, Escobar-Briones E, Gelinas Y, Menot L, Sarrazin J (2016) Food-Web Complexity in Guaymas Basin Hydrothermal Vents and Cold Seeps. PLoS One 11:e0162263
R Core Team (2013) R: A Language and environment for statistical computing. R Foundation for Statistical Computing, Vienna, Austria http://www.R-project.org/.
Rau GH (1981) Low $^{15}N/^{14}N$ in hydrothermal vent animals: ecological implications. Nature 289:484-485
Reid WDK, Sweeting CJ, Wigham BD, Zwirglmaier K, Hawkes JA, McGill RAR, Linse K, Polunin NVC (2013) Spatial Differences in East Scotia Ridge Hydrothermal Vent Food Webs: Influences of Chemistry, Microbiology and Predation on Trophodynamics. Plos One 8
Reid WDK, Wigham BD, McGill RAR, Polunin NVC (2012) Elucidating trophic pathways in benthic deep-sea assemblages of the Mid-Atlantic Ridge north and south of the Charlie-Gibbs Fracture Zone. Marine Ecology Progress Series 463:89-103
Rennie MD, Ozersky T, Evans DO (2012) Effects of formalin preservation on invertebrate stable isotope values over decadal time scales. Canadian Journal of Zoology 90:1320-1327
Rodrigues CF, Hilário A, Cunha MR (2013) Chemosymbiotic species from the Gulf of Cadiz (NE Atlantic): distribution, life styles and nutritional patterns. Biogeosciences 10:2569-2581
Sahling H, Wallman K, Dählmann A, Schmaljohann R, Petersen S (2005) The physicochemical habitat of *Sclerolinum sp.* at Hook Ridge hydrothermal vent, Bransfield Strait, Antarctica. Limnology & Oceanography 50:598-606
Schlesner H (2015) Blastopirellula. Bergey's Manual of Systematics of Archaea and Bacteria. John Wiley & Sons, Ltd
Schmaljohann R, Faber E, Whiticar MJ, Dando PR (1990) Co-existence of methane- and sulphur-based endosymbioses between bacteria and invertebrates at a site in the Skagerrak. Marine Ecology Progress Series 61:11-124
Schmaljohann R, Flügel HJ (1987) Methane-oxidizing bacteria in Pogonophora. Sarsia 72:91-98
Sellanes J, Zapata-Hernández G, Pantoja S, Jessen GL (2011) Chemosynthetic trophic support for the benthic community at an intertidal cold seep site at Mocha Island off central Chile. Estuarine, Coastal and Shelf Science 95:431-439
Soto LA (2009) Stable carbon and nitrogen isotopic signatures of fauna associated with the deep-sea hydrothermal vent system of Guaymas Basin, Gulf of California. Deep Sea Research Part II: Topical Studies in Oceanography 56:1675-1682
Southward A, J., Southward EC, Brattegard T, Bakke T (1979) Further Experiments on the value of Dissolved Organic Matter as Food for *Siboglinum fjiordicum* (Pogonophora). Journal of Marine Biological Asociation of the United Kingdom 59:133-148
Sweetman AK, Levin LA, Rapp HT, Schander C (2013) Faunal trophic structure at hydrothermal vents on the southern Mohn's Ridge, Arctic Ocean. Marine Ecology Progress Series 473:115
Tarasov VG, Gebruk AV, Mironov AN, Moskalev LI (2005) Deep-sea and shallow-water hydrothermal vent communities: Two different phenomena? Chemical Geology 224:5-39
Teske A, Callaghan AV, LaRowe DE (2014) Biosphere frontiers of subsurface life in the sedimented hydrothermal system of Guaymas Basin. Frontiers in microbiology 5:362
Teske A, Hinrichs KU, Edgcomb V, de Vera Gomez A, Kysela D, Sylva SP, Sogin ML, Jannasch HW (2002) Microbial Diversity of Hydrothermal Sediments in the Guaymas Basin: Evidence for Anaerobic Methanotrophic Communities. Applied and environmental microbiology 68:1994-2007

968 Thornhill DJ, Wiley AA, Campbell AL, Bartol FF, Teske A, Halanych KM (2008) Endosymbionts of
969 *Siboglinum fjordicum* and the Phylogeny of Bacterial Endosymbionts in Siboglinidae
970 (Annelida). Biological Bulletin 214:135-144
971 Thornton B, Zhang Z, Mayes RW, Högberg MN, Midwood AJ (2011) Can gas chromatography
972 combustion isotope ratio mass spectrometry be used to quantify organic compound
973 abundance? Rapid Communications in Mass Spectrometry 25:2433-2438
974 Tyler PA, Connelly DP, Copley JT, Linse K, Mills RA, Pearce DA, Aquilina A, Cole C, Glover AG,
975 Green DR, Hawkes JA, Hepburn L, Herrera S, Marsh L, Reid WD, Roterman CN, Sweeting
976 CJ, Tate A, Woulds C, Zwirglmaier K (2011) RRS *James Cook* cruise JC55: Chemosynthetic
977 Ecosystems of the Southern Ocean. BODC Cruise Report
978 Valls M, Olivar MP, Fernández de Puelles ML, Molí B, Bernal A, Sweeting CJ (2014) Trophic
979 structure of mesopelagic fishes in the western Mediterranean based on stable isotopes of
980 carbon and nitrogen. Journal of Marine Systems 138:160-170
981 Vetter RD, Fry B (1998) Sulfur contents and sulfur-isotope compositions of thiotrophic
982 symbioses in bivalve molluscs and vestimentiferan worms. Marine Biology 132:453-460
983 Veuger B, van Oevelen D, Middelburg JJ (2012) Fate of microbial nitrogen, carbon, hydrolysable
984 amino acids, monosaccharides, and fatty acids in sediment. Geochimica Et Cosmochimica
985 Acta 83
986 Walker BD, McCarthy MD, Fisher AT, Guilderson TP (2008) Dissolved inorganic carbon isotopic
987 composition of low-temperature axial and ridge-flank hydrothermal fluids of the Juan de
988 Fuca Ridge. Marine Chemistry 108:123-136
989 Wang Q, Garrity GM, Tiedje JM, Cole JR (2007) Naïve Bayesian Classifier for Rapid Asssignment
990 of rRNA sequences into the New Bacterial Taxonomy. Applied Environmental
991 Microbiology 73:5261-5267
992 Whitaker D, Christmann M (2013) Package 'clustsig'. cranr-projectorg
993 Whiticar MJ (1999) Carbon and Hydrogen isotope systematics of bacterial formation and
994 oxidation of methane. Chemical Geology 161:291-314
995 Whiticar MJ, Suess E (1990) Hydrothermal hydrocarbon gases in the sediments of the King
996 George Basin, Bransfield Strait, Antarctica. Applied Geochemistry 5:135-147
997 Woolley SNC, Tittensor DP, Dunstan PK, Guillera-Arroita G, Lahoz-Monfort JJ, Wintle BA, Worm
998 B, O'Hara TD (2016) Deep-sea diversity patterns are shaped by energy availability.
999 Nature
1000 Wu Y, Cao Y, Wang C, Wu M, Aharon O, Xu X (2014) Microbial community structure and
1001 nitrogenase gene diversity of sediment from a deep-sea hydrothermal vent field on the
1002 Southwest Indian Ridge. Acta Oceanologica Sinica 33:94-104
1003 Würzberg L, Peters J, Schüller M, Brandt A (2011) Diet insights of deep-sea polychaetes derived
1004 from fatty acids analyses. Deep Sea Research Part II 58:153-162
1005 Yamanaka T, Sakata S (2004) Abundance and distribution of fatty acids in hydrothermal vent
1006 sediments of the western Pacific Ocean. Organic Geochemistry 35:573-582
1007 Yamanaka T, Shimamura S, Nagashio H, Yamagami S, Onishi Y, Hyodo A, Mampuku M, Mizota C
1008 (2015) A Compilation of the Stable Isotopic Compositions of Carbon, Nitrogen, and Sulfur
1009 in Soft Body Parts of Animals Collected from Deep-Sea Hydrothermal Vent and Methane
1010 Seep Fields: Variations in Energy Source and Importance of Subsurface Microbial
1011 Processes in the Sediment-Hosted Systems. In: Ishibashi J, Okino K, Sunamura M (eds)
1012 Subseafloor Biosphere Linked to Hydrothermal Systems. SpringerOpen, Tokyo
1013 Yorisue T, Inoue K, Miyake H, Kojima S (2012) Trophic structure of hydrothermal vent
1014 communities at Myojin Knoll and Nikko Seamount in the northwestern Pacific:
1015 Implications for photosynthesis-derived food supply. Plankton and Benthos Research
1016 7:35-40

1017 Young JN, Bruggeman J, Rickaby REM, Erez J, Conte M (2013) Evidence for changes in carbon
1018 isotopic fractionation by phytoplankton between 1960 and 2010. Global Biogeochemical
1019 Cycles 27:505-515
1020

1021

10. Figure captions

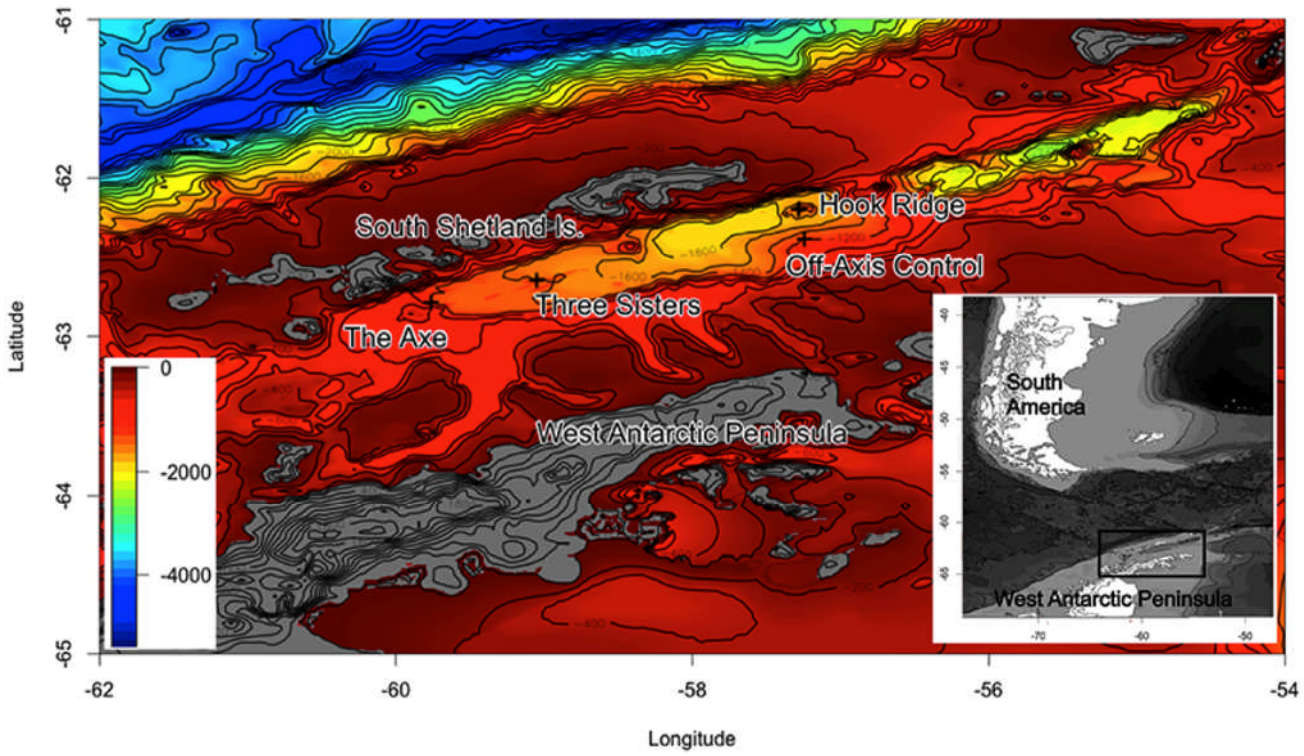

Figure 1 – Sampling sites (after Bell et al. 2016b)

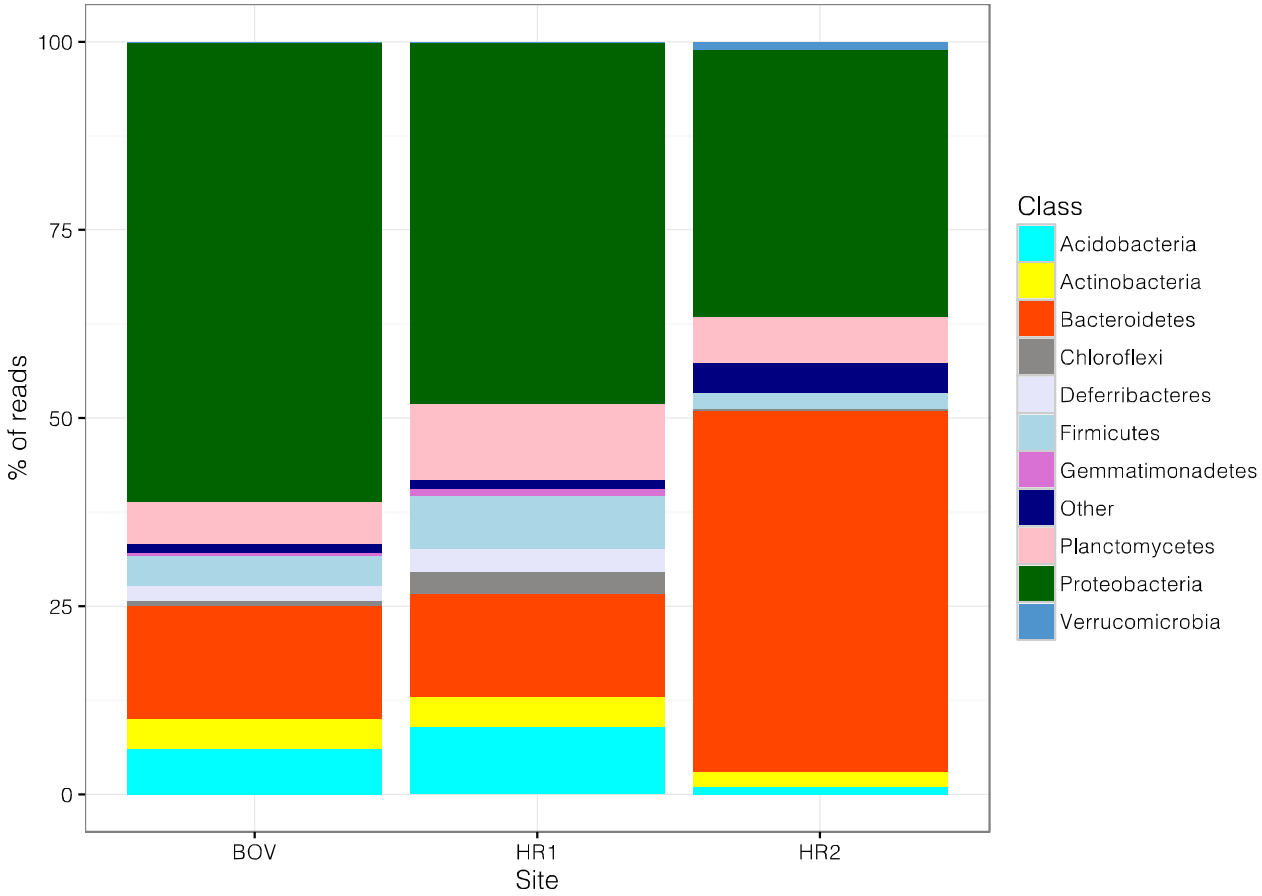

Figure 2 – Microbial composition (classes) at the off-vent/ off-axis site (BOV) and the two Hook Ridge sites (HR1 and HR2). Archaea excluded from figure as they only accounted for 0.008 % of reads at HR2 and were not found elsewhere.

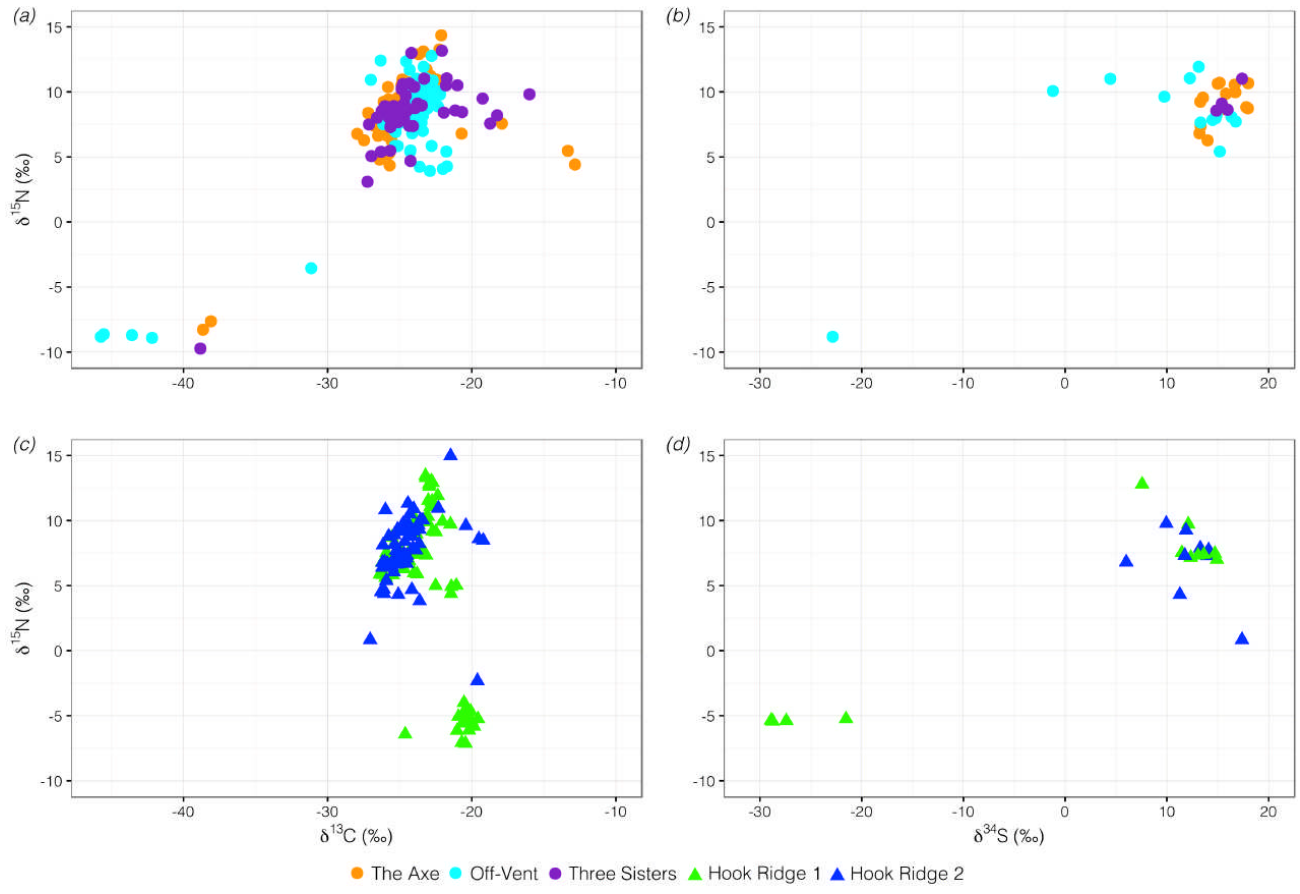

1031

1032 Figure 3 – Carbon-Nitrogen and Sulphur-Nitrogen biplots for bulk isotopic signatures of benthos,
1033 separated into non-hydrothermal (top) and hydrothermal sites (bottom). Excepting one value
1034 from the off-vent site (for a peracarid species), all values with $\delta^{15}N$ of < 0 were siboglinid species
1035 (*Sclerolinum contortum* from the hydrothermal sites and *Siboglinum* spp. from the non-
1036 hydrothermal sites).

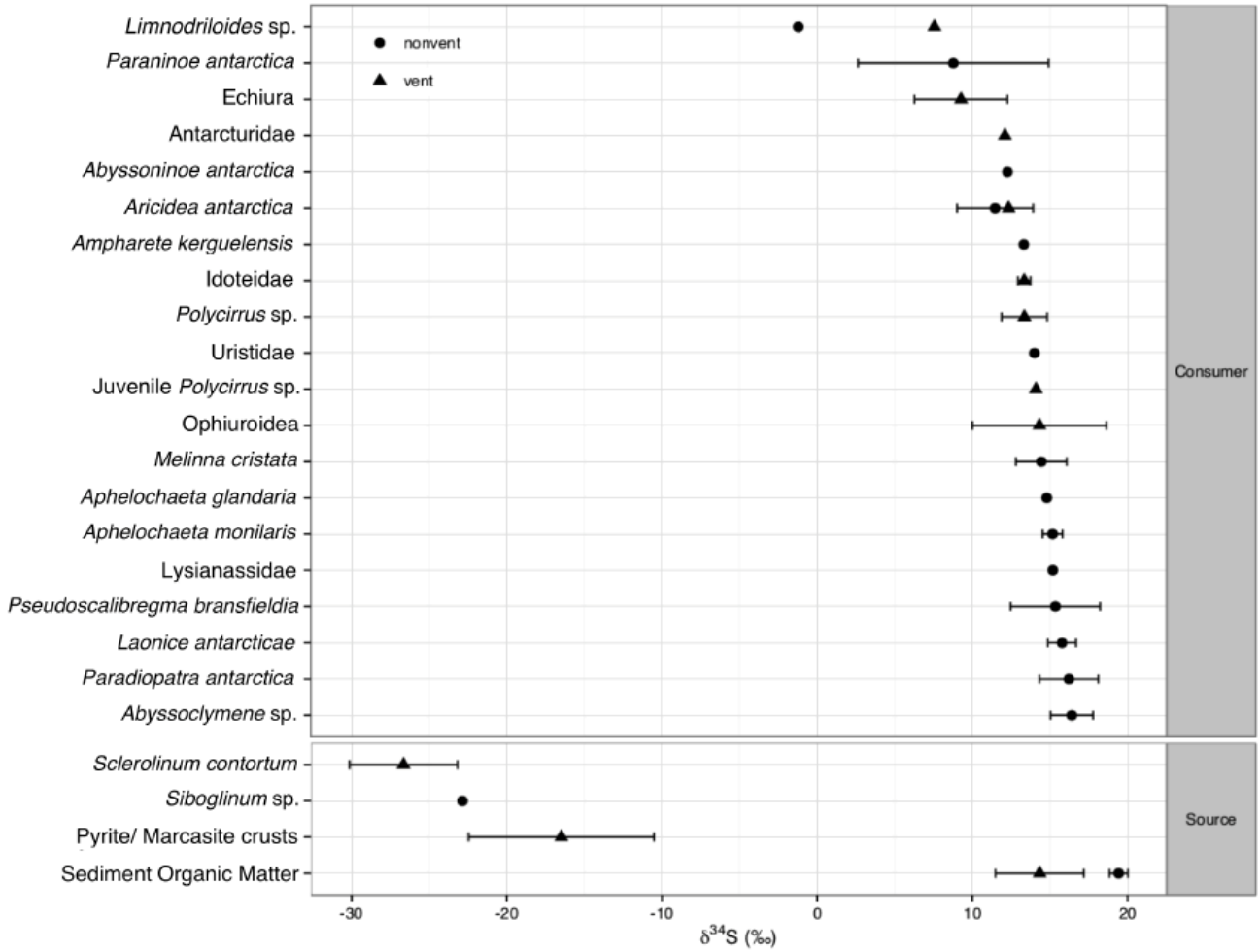

Figure 4 – Plot of $\delta^{34}S$ measurements by discriminated by species and habitat (hydrothermally active vents & sediments/ non-hydrothermally active sediments ± 1 s.d.). Data for $\delta^{34}S$ in crusts from Petersen et al. (2004)

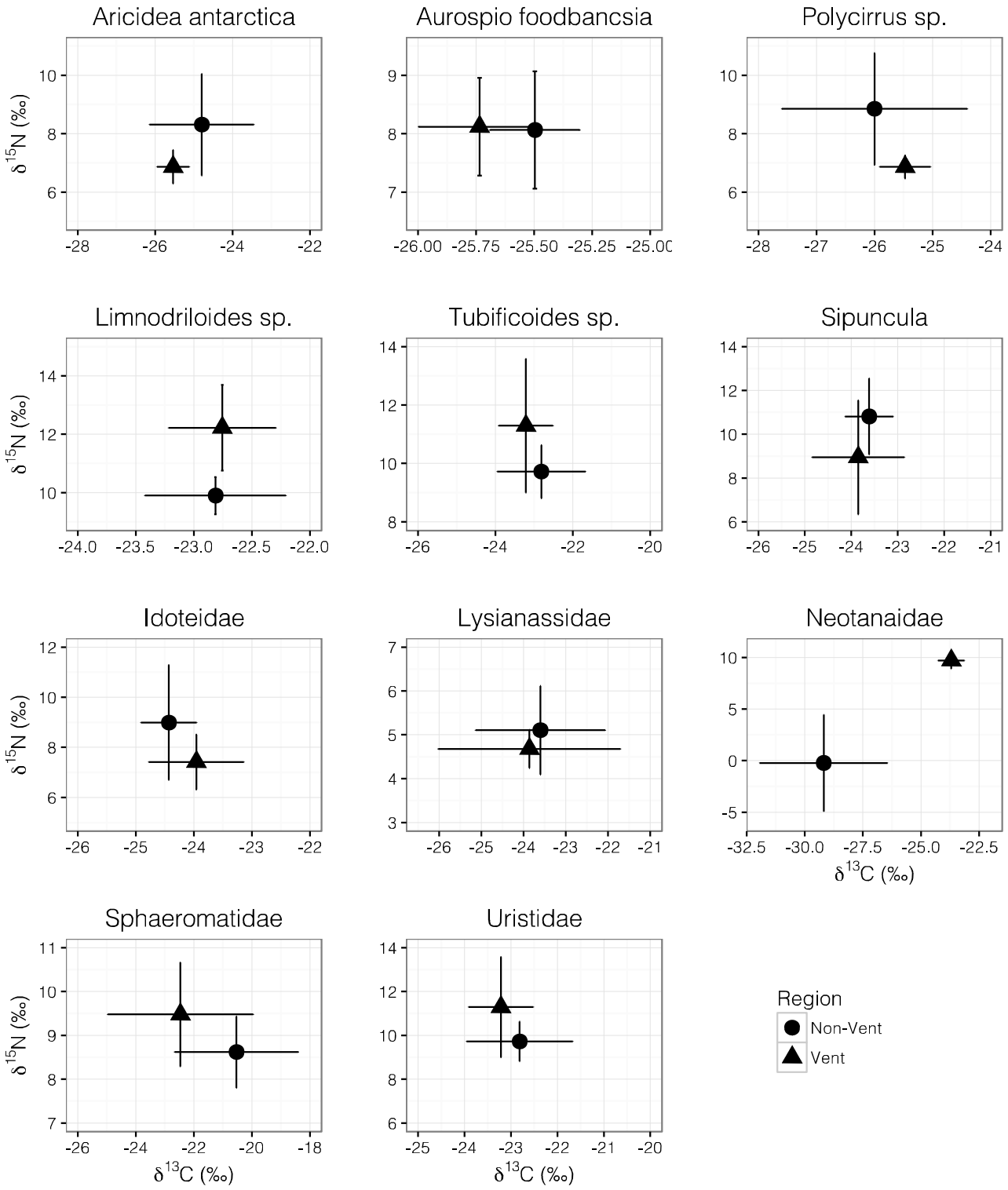

Figure 5– Biplot of CN isotopic data from species sampled both at hydrothermal sitess and non-hydrothermal background regions. Mean ± standard deviation, X-Y scales vary

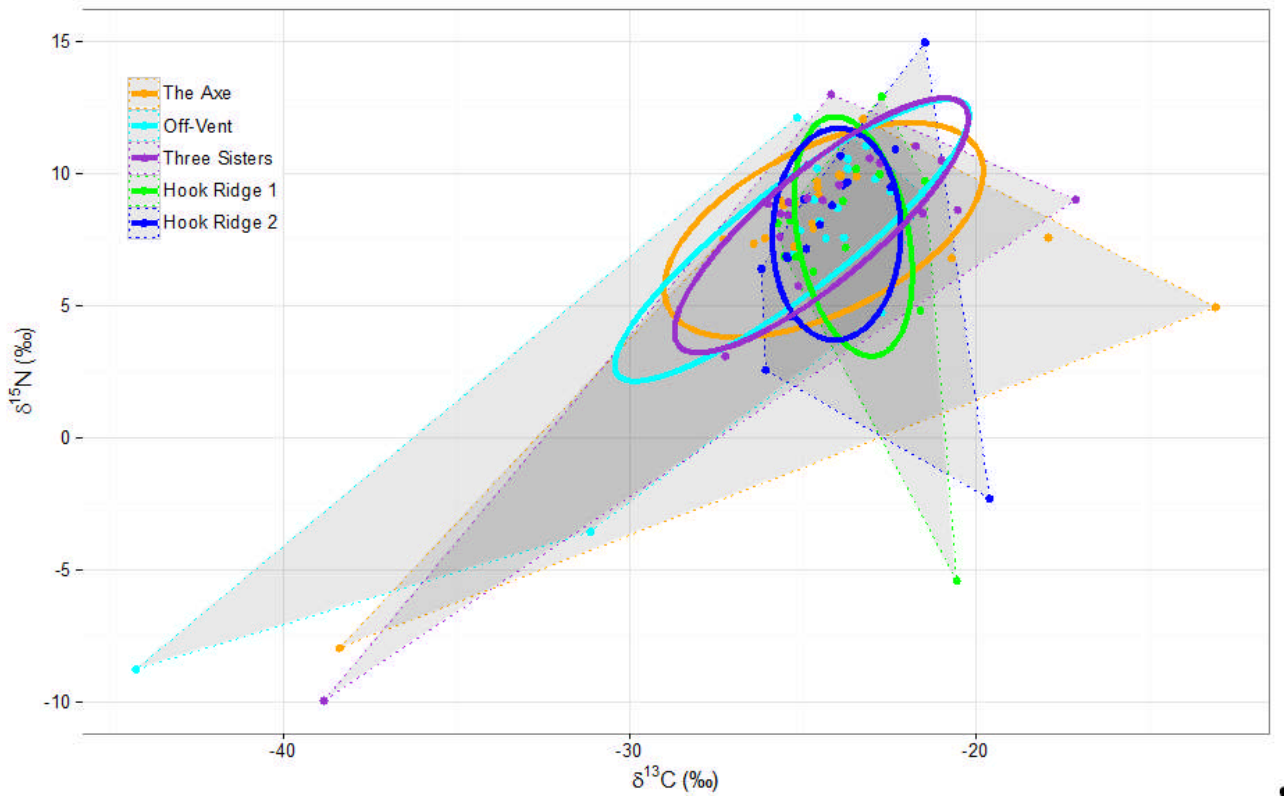

Figure 6 – Faunal isotopic signatures (mean per species), grouped by site with total area (shaded area marked by dotted lines) and sample-size corrected standard elliptical area (solid lines)

1052 11. Tables

Site	Depth (m)	Hydrothermally active?	References
The Axe (AXE)	1024	No	(Dählmann et al. 2001, Klinkhammer et al. 2001, Sahling et al. 2005, Aquilina et al. 2013, Aquilina et al. 2014, Bell et al. 2016b)
Off-Vent (BOV)	1150	No	
Three Sisters (TS)	1311	No	
Hook Ridge 1 (HR1)	1174	Low activity (9 cm yr^{-1})	
Hook Ridge 2 (HR2)	1054	High Activity (34 cm yr^{-1})	

1053

1054 Table 1 – Site descriptions and associated references

Isotope	Species	Idoteidae	*Polycirrus* sp.	*Aphelochaeta glandaria*	Phyllodocida sp.
	Treatment	0.1M HCl	0.1M HCl	0.1M HCl	1.0M HCl
$\delta^{13}C$ (‰)	Difference in mean	1.6	0.2	0.4	0.9
	σ untreated	0.7	0.3	0.2	0.5
	σ treated	0.7	0.3	0.2	0.2
	Population range	2.9	3.0	2.7	-
$\delta^{15}N$ (‰)	Difference in mean	0.9	0.2	0.1	0.9
	σ untreated	0.2	0.3	0.2	0.4
	σ treated	1.0	0.2	0.2	0.3
	Population range	3.4	4.6	5.8	-
$\delta^{34}S$ (‰)	Difference in mean	-	-	0.4	1.1
	σ untreated	-	-	0.4	0.8
	σ treated	-	-	0.7	1.4
	Population range	-	-	2.3	-

Table 2 – Differences in isotopic values and standard deviation (σ) of ethanol preserved fauna sampled during JC55 in response to acid treatment, compared with population ranges of untreated samples. Phyllodocida sp. was a single large specimen, used only as part of preliminary experiments. Data rounded to 1 d.p. to account for measurement error.

Genera	Class	Off-Vent %	Hook Ridge 1 %	Hook Ridge 2 %
Aestuariicola	Flavobacteria	1.37	0.53	6.89
Arenicella	Gammaproteobacteria	7.14	5.17	2.24
Blastopireulla	Planctomycetacia	2.50	3.01	1.92
Denitrovibiro	Deferribacteres	1.72	2.54	0.27
Geothermobacter	Deltaproteobacteria	2.40	1.90	0.52
Lutimonas	Flavobacteria	0.45	0.42	4.87
Maritimimonas	Flavobacteria	1.10	0.15	4.32
Methylohalomonas	Gammaproteobacteria	4.29	2.78	2.08
Pasteuria	Bacilli	3.30	5.02	1.67
Tenacibaculum	Flavobacteria	0.26	0.04	3.36
Winogradskyella	Flavobacteria	0.99	0.90	4.09

1062

1063

1064 Table 3 – Most dominant bacterial genera (covering the top 5 at each site), with percent of total

1065 sequenced reads.

1066

	Bransfield Off-Vent			**Three Sisters**		
PLFA	**nM g^{-1}**	**%**	**$\delta^{13}C$ (‰)**	**nM g^{-1}**	**%**	**$\delta^{13}C$ (‰)**
i14:0	0.03	0.12	-22.0	0.02	0.09	-28.0
14:0	0.80	3.04	-31.2	0.83	3.43	-30.9
i15:0	0.76	2.89	-28.6	0.76	3.13	-28.1
a15:0	1.06	4.03	-28.4	1.06	4.39	-27.7
15:0	0.30	1.13	-29.3	0.19	0.77	-29.8
i16:1	0.11	0.44	-31.4	0.02	0.10	-20.3

16:1w11c	0.00	0.00	n.d.	0.06	0.24	-23.1
i16:0	0.34	1.30	-28.5	0.30	1.24	-27.8
16:1w11t	0.78	2.98	-24.4	0.66	2.75	-25.0
16:1w7c	3.98	15.19	-28.9	3.37	13.95	-28.1
16:1w5c	1.12	4.27	-34.1	0.96	3.99	-34.0
16:0	4.29	16.37	-31.1	3.80	15.73	-30.0
br17:0	0.00	0.00	n.d.	0.00	0.00	n.d.
10-Me-16:0	0.46	1.77	-28.5	0.45	1.87	-29.1
i17:0	0.08	0.32	-33.2	0.20	0.84	-29.8
a17:0	0.25	0.97	-31.9	0.21	0.87	-31.3
12-Me-16:0	0.25	0.94	-32.9	0.21	0.86	-31.6
17:1w8c	0.13	0.50	-34.1	0.11	0.44	-31.3
17:0cy	0.33	1.26	-36.2	0.27	1.10	-32.8
17:0	0.15	0.56	-40.0	0.08	0.33	-50.4
10-Me-17:0	0.00	0.00	n.d.	0.00	0.00	n.d.
18:3w6,8,13	0.67	2.55	-34.6	0.69	2.87	-33.8
18:2w6,9	0.12	0.46	-27.8	0.09	0.36	-52.2
18:1w9	1.13	4.30	-30.0	1.33	5.50	-29.9
18:1w7	4.42	16.85	-29.0	3.84	15.91	-29.1
18:1w(10 or 11)	2.33	8.88	-30.1	2.26	9.36	-29.9
18:0	0.66	2.50	-30.6	0.54	2.22	-30.6
19:1w6	0.03	0.12	-23.5	0.03	0.12	-30.1
10-Me-18:0	0.00	0.00	n.d.	0.00	0.00	n.d.
19:1w8	0.11	0.42	-56.6	0.17	0.69	-37.5
19:0cy	0.20	0.77	-35.6	0.20	0.83	-34.8
20:4(n-6)	0.14	0.55	-40.0	0.20	0.83	-34.1
20:5(n-3)	0.41	1.57	-38.0	0.30	1.23	-39.3
20:1(n-9)	0.42	1.60	-31.5	0.41	1.71	-33.7
22:6(n-3)	0.22	0.83	-34.1	0.43	1.77	-30.0
22:1(n-9)	0.10	0.39	-31.3	0.10	0.41	-29.9
24:1(n-9)	0.03	0.12	-28.7	0.02	0.07	-29.7
Total	26.23			24.15		
Average	0.71		-30.5	0.65		-30.1
		mg C m^{-2}	**$\delta^{13}C$ (‰)**		**mg C m^{-2}**	**$\delta^{13}C$ (‰)**
Bacterial Biomass		134.50	-26.8		197.12	-26.4

1067

1068

	Hook Ridge 1		**Hook Ridge 2**			**Range**
PLFA	**nM g^{-1}**	**$\delta^{13}C$ (‰)**	**nM g^{-1}**	**%**	**$\delta^{13}C$ (‰)**	**$\delta^{13}C$**

						(‰)
i14:0	0.03	-15.7	0.10	0.80	-28.8	-13.1
14:0	0.80	-32.7	0.80	6.40	-29.6	-3.1
i15:0	0.76	-29.7	0.40	3.20	-28.1	-1.7
a15:0	1.06	-29.1	0.90	7.20	-28.9	-1.4
15:0	0.30	-29.0	0.30	2.40	-28.3	-1.5
i16:1	0.11	-27.6	0.00	0.00	n.d.	-11.1
16:1ω11c	0.00	-17.4	0.00	0.00	n.d.	-5.7
i16:0	0.34	-29.4	0.20	1.60	-28.8	-1.6
16:1ω11t	0.78	-25.8	0.30	2.40	-8.7	-17.2
16:1ω7c	3.98	-29.2	2.50	20.00	-22.9	-6.3
16:1ω5c	1.12	-31.2	0.30	2.40	-24.3	-9.7
16:0	4.29	-31.8	3.30	26.40	-29.3	-2.5
br17:0	0.00	-22.9	0.00	0.00	-15.8	-7.2
10-Me-16:0	0.46	-30.3	0.20	1.60	-41.3	-12.8
i17:0	0.08	n.d.	0.00	0.00	n.d.	-3.4
a17:0	0.25	-29.0	0.20	1.60	-28.6	-3.4
12-Me-16:0	0.25	-28.6	0.10	0.80	-28.2	-4.7
17:1ω8c	0.13	-27.1	0.10	0.80	-27.2	-6.9
17:0cy	0.33	-32.3	0.20	1.60	-27.7	-8.5
17:0	0.15	-40.0	0.20	1.60	-30.8	-19.6
10-Me-17:0	0.00	-35.0	0.00	0.00	n.d.	0.00
18:3ω6,8,13	0.67	-31.2	0.50	4.00	-29.0	-5.6
18:2ω6,9	0.12	-30.0	0.30	2.40	-26.7	-25.5
18:1ω9	1.13	-29.6	0.40	3.20	-25.6	-4.4
18:1w7	4.42	-29.9	0.60	4.80	-24.7	-5.1
18:1ω(10 or 11)	2.33	-31.9	0.00	1.60	n.d.	-2.0
18:0	0.66	-29.4	0.30	0.00	-29.9	-1.2
19:1ω6	0.03	-26.2	0.00	2.40	n.d.	-6.6
10-Me-18:0	0.00	-25.4	0.00	0.00	n.d.	0.0
19:1ω8	0.11	-41.2	0.00	0.00	n.d.	-19.1
19:0cy	0.20	-30.5	0.10	0.00	-28.7	-6.9
20:4(n-6)	0.14	n.d.	0.00	0.80	n.d.	-5.9
20:5(n-3)	0.41	n.d.	0.00	0.00	n.d.	-1.3
20:1(n-9)	0.42	n.d.	0.00	0.00	n.d.	-2.2
22:6(n-3)	0.22	n.d.	0.00	0.00	n.d.	-4.2
22:1(n-9)	0.10	n.d.	0.00	0.00	n.d.	-1.4
24:1(n-9)	0.03	n.d.	0.00	0.00	n.d.	-1.0

Total	26.23		12.30			
Average	0.71	-30.3	0.33		-26.9	
	mg C m^{-2}	**$\delta^{13}C$ (‰)**		**mg C m^{-2}**	**$\delta^{13}C$ (‰)**	
Bacterial Biomass	534.55	-26.6		85.45	-23.1	

1069

1070 Table 4 – PLFA profiles from freeze-dried sediment (nM per g dry sediment). PLFA names relate
1071 to standard notation (i = iso; a = anti-iso; first number = number of carbon atoms in chain; ω =
1072 double bond; Me = methyl group). N.P. = Not present in sample. Total PLFA $\delta^{13}C$ measurements
1073 weighted by concentration Bulk bacterial $\delta^{13}C$ estimated from average conversion factor of
1074 3.7 ‰ (Boschker & Middelburg 2002). No data = n.d. Range measurements may be subject to
1075 rounding error. N. B. Table split to conform to submission portal requirements.

1076

1077

Isotope	Hydrothermal sites ‰ (± S.D.)	Non-Hydrothermal sites ‰ (± S.D.)	Different? (T-Test, df = 3)
$\delta^{13}C$	-26.2 (± 0.4)	-25.8 (± 0.3)	No
$\delta^{15}N$	5.7 (± 0.7)	5.0 (± 0.3)	No
$\delta^{34}S$	14.3 (± 2.9)	19.4 (± 0.6)	Yes ($T = 3.49$, $p < 0.05$)

1078

1079 Table 5 – Mean isotopic signatures of sediment organic matter.

1080

	Ellipse							Nearest Neighbour Distance	
Site	**SEAc (‰²)**	**SEA.B (‰²)**	**Cred. (95% ± ‰²)**	**TA (‰²)**	**Θ**	**E**	**CD**	**Mean**	**S.D.**
The Axe	49.3	45.0	19.9	161.6	0.67	0.85	3.59	1.76	4.17
Off-Vent	39.8	36.5	16.8	139.1	0.81	0.97	4.34	2.13	3.88
Three Sisters	35.5	32.6	14.7	110.2	0.86	0.95	3.85	1.93	3.78
Hook Ridge 1	23.1	20.7	11.2	42.6	-1.43	0.94	3.30	1.64	2.60
Hook Ridge 2	23.4	21.1	10.7	61.8	1.55	0.89	3.17	1.52	2.03
Mean									
Non-Hydrothermal	**41.5**	**38.0**	**17.2**	**137.0**	**0.78**	**0.92**	**3.93**	**1.94**	**3.94**
Hydrothermally active	**23.2**	**20.9**	**11.0**	**52.2**	**0.10**	**0.91**	**3.23**	**1.58**	**2.31**

1081

	Centroid				
Site	**$\delta^{13}C$ (‰)**	**$\delta^{15}N$ (‰)**	**$\delta^{34}S$ (‰)**	**dNr (‰)**	**dCr (‰)**
The Axe	-24.4	7.9		20.0	25.3
Off-Vent	-25.3	7.5	8.1	20.9	22.7

Three Sisters	-24.5	8.0		22.9	21.7
Hook Ridge 1	-23.5	7.6	5.4	18.3	5.2
Hook Ridge 2	-24.0	7.7		17.3	6.6
Mean					
Non-Hydrothermally active	**-24.7**	**7.8**		**21.3**	**23.2**
Hydrothermally active	**-23.8**	**7.7**		**17.8**	**5.9**

Table 6 – Ellipse Area & Layman Metrics of benthos by site. SEAc = Sample-sized corrected standard elliptical area; SEA.B = Bayesian estimate of standard elliptical area; TA = Total hull area; E = Eccentricity; dNr = Nitrogen range; dCr = Carbon range; dSr = Sulphur range; CD = Centroid distance. Note: dSR reported only for Hook Ridge 1 and the off-vent site since $\delta^{34}S$ values of siboglinids were only measured from these sites; hence dSr at other sites would be a considerable underestimate. As $\delta^{34}S$ values were comparatively under-representative, these values were not used in calculation of any other metric. Data rounded to 1 d.p. N. B. Table split to conform to submission portal requirements.

Supplementary Information

Supplementary Figure 1 – PLFA Abundances by site.

Supplementary Figure 2 – nMDS plot of PLFA composition, with reference to PLFA suites from the Goban Spur (NE Atlantic) (Main et al. 2015) and Loki's Castle hydrothermal sediments (Jaeschke et al. 2014).

Supplementary Figure 3 – Cluster dendrogram (Euclidean distance) for averaged CN isotopic signatures for species from vent and non-vent areas.

Supplementary File 1 – Bulk isotopic data.

Supplementary File 2 – PLFA data.